Effect of Environmental Stress and Bias Conditions on Reliability of Embedded Planar Capacitors

Mohammed Alam[1], Michael H. Azarian[1], Michael Osterman[1] and Michael Pecht[1, 2]

[1]Center for Advanced Life Cycle Engineering (CALCE)
University of Maryland, College Park, MD 20742

[2]Prognostics and Health Management Center
City University of Hong Kong, Kowloon, Hong Kong
Corresponding Author: mgpecht@cityu.edu.hk

Abstract

The reliability of an embedded planar capacitor laminate under a variety of environmental stress and bias conditions was investigated. The dielectric consisted of a composite of $BaTiO_3$ particles in a bisphenol-epoxy matrix. The capacitor laminate was embedded in a 4-layer test board in which the power plane was etched to form discrete embedded capacitors having a common ground plane. Capacitors of two different areas were studied, having capacitances of about 400 pF and 5 nF.

The test vehicle with embedded capacitors was subjected to temperature and voltage aging and temperature-humidity-bias (THB) tests at different stress levels. Three parameters, capacitance (C), dissipation factor (DF), and insulation resistance (IR), were measured in-situ during stress testing. Results are presented of testing at multiple stress levels in temperature and voltage aging tests and THB testing. Changes in electrical parameters during stress testing are reported, as well as the effects of stress conditions and levels on characteristic life. Physical analysis is used to identify the material response of the embedded capacitor laminate to the imposed stresses, providing the basis for recommendations regarding laminate design and usage.

1 Introduction

Embedded planar capacitors are thin laminates that serve both as a power/ground plane and as a parallel plate capacitor in a multilayered printed wiring board (PWB). These laminates can be embedded throughout the board, eliminating the need for discrete surface mount capacitors (which are used for decoupling) to be adjacent to an integrated circuit (IC). Board space taken up by discrete surface mount capacitors and their corresponding interconnections can be saved, and that can allow miniaturization of the PWBs. Due to the lower number of solder joints the reliability of the board is expected to improve, provided the embedded capacitors have sufficient reliability. Embedded capacitors have also been found to reduce high frequency electromagnetic interference (EMI) as compared to discrete surface mount capacitors [1]. The key to the reduction in the number of surface mount capacitors is the low value of inductance associated with embedded capacitors due to elimination of leads and traces and the thinness of the dielectric [2].

The laminate for an embedded capacitor consists of a thin dielectric sandwiched between copper layers. The dielectric material can be a polymer or a composite of polymer and high dielectric constant ceramic (when a high dielectric constant is required). The dielectric material can also be polymer reinforced with glass fibers to provide mechanical strength. The dielectric material investigated in this work is a polymer-high dielectric constant ceramic composite. The advantage of using a composite is that it combines low temperature processability of polymers with the high dielectric constant available in certain ceramics [1]. The polymer typically used is epoxy, although polyimide is used for high temperature applications. A commonly used high dielectric constant ceramic is barium titanate ($BaTiO_3$), which can have a dielectric constant as high as 15,000 [3]. The dielectric constant of $BaTiO_3$ is at its maximum when the particle size is close to 140 nm [4], so nano-particles of $BaTiO_3$ are preferred. With an increase in the ceramic loading the dielectric constant of the composite increases according to the relation [5]:

$$\log \varepsilon_c = V_m \log \varepsilon_m + V_p \log \varepsilon_p \tag{1}$$

where ε_c is the dielectric constant of the composite, ε_m is the dielectric constant of the polymer matrix, ε_p is the dielectric constant of the ceramic, V_m is the volume fraction of the polymer, and V_p is the volume fraction of the ceramic. The above equation is not valid beyond 55-60% of ceramic loading by volume, when the theoretical maximum packing density is exceeded and the dielectric constant decreases due to an increase in voids and pores in the composite [6]. Typically, for reliability reasons the maximum ceramic loading is lower than 50% by volume, which limits the maximum dielectric constant of the composite close to 30 [7].

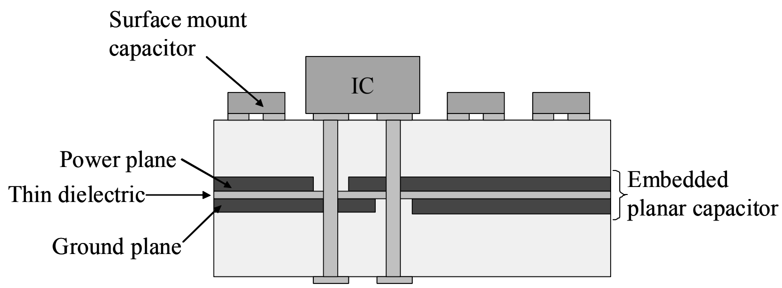

Fig. 1. Embedded planar capacitor

Embedded capacitors have many advantages, but the reliability of these capacitors will determine the breadth and success of their practical application. A drift in the electrical parameters (such as capacitance, dissipation factor, and insulation resistance) of an embedded planar capacitor can affect the performance of the circuit where these capacitors are used. Since embedded capacitors are not reworkable, the entire PWB will have to be scrapped if these capacitors are not functioning properly. The failure mode can be a drift in capacitance, dissipation factor, or insulation resistance beyond permissible limits (which can be defined depending on the application). Possible failure modes and mechanisms due to temperature and voltage aging and temperature-humidity-bias (THB) are discussed in this paper. Accelerated temperature and voltage aging and THB tests were conducted at various stress levels, and three parameters, capacitance, dissipation factor, and insulation resistance, were monitored in-situ.

2 Effect of temperature and voltage on electrical properties

The electrical parameters of an embedded capacitor, such as capacitance and insulation resistance, can change due to temperature and voltage. The capacitance can decrease due to an increase in the spacing between the plates due to thermal deformation and delamination in the capacitor laminate. These phenomena are driven by the thermo-mechanical stresses developed at the dielectric-Cu plane interface due to a difference between the coefficient of thermal expansion (CTE) of the dielectric and the Cu plane [8]. Possible sources of thermal stresses can be variations in the ambient temperature and solder reflow.

Another possible mechanism of decrease in capacitance is aging in the $BaTiO_3$ [9], which is a gradual decrease in the dielectric constant after the dielectric's last excursion beyond the Curie temperature (about 130°C for $BaTiO_3$). Aging can be described by the well-known equation [10]:

$$\frac{C}{C_o} = 1 - k[\log(t)] \qquad (2)$$

where C is the capacitance after time t, C_0 is the initial capacitance, k is the dielectric aging rate, and t is the time. Capacitors can be restored to their original capacitance by heating them above their Curie temperature for a period of time. The aging rate increases with an increase in the temperature [11].

Residual stress relaxation in the polymer matrix can also cause a drop in the capacitance [12]. The residual stresses in the polymer matrix generated during curing can be relaxed by exposure to temperatures above the glass transition temperature (T_g) of the polymer. Due to stress relaxation the polymer chains can move more freely, and their free volume increases. An increase in free volume leads to a decrease in the dielectric constant, since the dielectric constant of free volume is equal to 1.0.

Insulation resistance can decrease due to voltage and temperature and is generally a concern in pure $BaTiO_3$ dielectric used in multilayer ceramic capacitors (MLCC). Typically there are two modes for a decrease in insulation resistance [13]. In the first mode, there is a sudden drop in insulation resistance, which is known as avalanche breakdown (ABD). In the second mode, there is a gradual decrease in the insulation resistance, which increases the self-heating due to an increase in the leakage current and is known as thermal runaway (TRA). The cause of ABD is attributed to extrinsic flaws in the dielectric such as porosity, delaminations, thin spots, cracks, local contamination, and voids. The cause of TRA in $BaTiO_3$ dielectric has been attributed to migration of oxygen vacancies in the presence of temperature and voltage [14]. These oxygen vacancies are created when $BaTiO_3$ dielectric is fired in reducing atmosphere (low oxygen partial pressure) [15].

An empirical model of time-to-failure as a result of drop in insulation resistance during temperature and voltage aging was proposed by Prokopowicz and Vaskas, and may be represented as [16]:

$$\frac{t_1}{t_2} = \left(\frac{V_2}{V_1}\right)^n \exp\left(\frac{E_a}{k}\left(\frac{1}{T_1} - \frac{1}{T_2}\right)\right) \qquad (3)$$

where t is the time-to-failure, V is the voltage, n is the voltage exponent, E_a is the activation energy, k is the Boltzmann constant, T is the temperature, and the subscripts *1* and *2* refer to the two aging conditions. This model is used in accelerated life tests of multilayer ceramic capacitors (MLCCs) to precipitate defects in the dielectric. There exists a lot of published work [15]-[21] on the computation of Prokopowicz model constants for pure $BaTiO_3$ dielectric used in MLCCs. But the values of these constants are not reported for a composite dielectric of epoxy and $BaTiO_3$ used in embedded capacitors. In this work, temperature and voltage aging tests will be performed at multiple stress levels to compute the values of these constants.

3 Effect of temperature, humidity, and bias on electrical properties

In the presence of elevated temperature and humidity, the capacitance of embedded capacitors (with epoxy-$BaTiO_3$ composite dielectric) has been found to increase due to moisture absorption in the dielectric [22][23]. The main site for moisture absorption in polymer-ceramic nanocomposites is the interface between the ceramic particle and the polymer matrix [24]. A decrease in the particle size (from the order of micrometers to nanometers) has been found [24] to increase the moisture absorption due to an increase in the interfacial area. Similarly, an increase in the ceramic loading (from 50% to 60% by volume) was found [5] to increase the moisture absorption due to an increase in the interfacial area. With a further increase in the ceramic loading beyond 60%, the moisture absorption was found to decrease as the interfacial area and the packing density approached the theoretical maximum. The increase in capacitance under humid conditions is reversible, and the capacitance has been observed to recover to its original value after a high temperature bake above 100^{o}C [12]. The effect of an applied voltage under elevated temperature and humidity conditions has not been reported in literature. An applied bias is expected to degrade the insulation resistance under humid conditions. In this study, THB tests were performed at various voltage levels while keeping the temperature and humidity constant to investigate the effect of an applied bias.

4 Test vehicle and experimental setup

The test vehicle in this study was a 4-layer PWB (shown in Fig. 2) in which layers 1 and 4 were the signal layers, and the planar capacitor laminate formed layer 2 (power plane) and layer 3 (ground plane). The power plane was etched at various locations to form discrete capacitors. Two types of square capacitors having an area of 0.026 in^2 and 0.19 in^2 were investigated in this work. There were 80 small capacitors (0.026 in^2) and 6 large capacitors (0.19 in^2) in the test vehicle, which are referred to as group A and group B respectively.

Each capacitor had its power plane connected to a plated through hole (PTH), as shown in Fig. 3. The ground plane was common for all capacitors and continuous as far as possible (except for the antipads). The dielectric was a composite of $BaTiO_3$ of mean diameter equal to 0.25 μm loaded 45% by volume in bisphenol-epoxy. The dielectric thickness was 8 μm and the dielectric constant of the composite was 16 at 1 KHz.

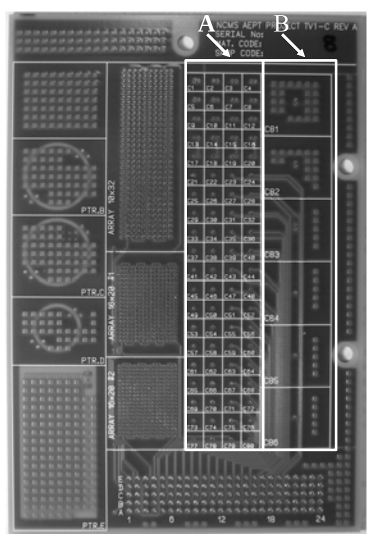

Fig. 2. Test vehicle of embedded capacitors

An experimental setup was designed for biasing the embedded capacitors in the test vehicle (which was kept in an environmental chamber). In this work, three parameters, capacitance, dissipation factor, and insulation resistance, were measured. The capacitance and dissipation factor were measured using an Agilent 4263B LCR meter at 100 KHz. Insulation resistance was measured with an Agilent 4339B high resistance meter by applying a bias of 10 V. The switching of individual capacitor channels for measurements was performed by an Agilent 34980A switching/measuring unit. In order to limit the current in a capacitor channel in case of a dielectric failure, a 1.1 MΩ resistor was added in series to each capacitor.

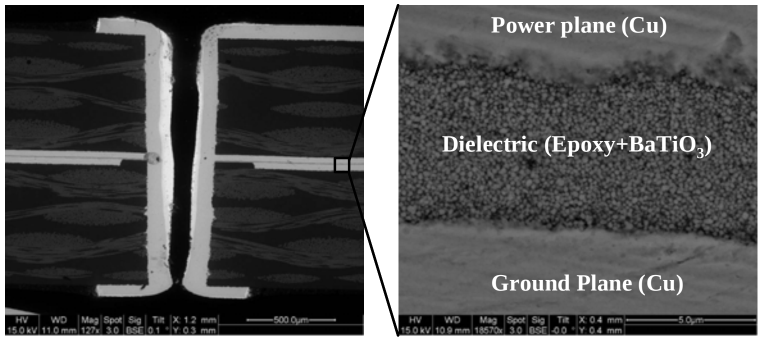

Fig. 3. Sectional view of an embedded capacitor

The failure criteria selected were a 20% decrease in capacitance, an increase in dissipation factor by a factor of 2, or a drop in insulation resistance to 1.1 MΩ (the value of the series resistor). The boards were preconditioned at 105°C for 48 hrs to drive off moisture before the start of the experiments.

5 Temperature and voltage aging

The objective of the temperature and voltage aging tests was to compute the values of constants (n and E_a) of the Prokopowicz model. The values of n and E_a can be used to calculate the acceleration factor applicable to temperature and voltage aging tests. A preliminary time-terminated temperature and voltage aging test was conducted at 125°C and 200V that lasted for 1000 hrs [25]. Measurements were performed on 33 capacitors of group A and 4 capacitors of group B. In the preliminary test, 5 out of 33 capacitors of group A and 4 out of 4 capacitors of group B failed due to a sharp drop in insulation resistance, indicating avalanche breakdown (ABD). The capacitance was found to decrease with time; however, the decrease was not significant enough to be considered a failure in both groups (A and B).

The number of failures due to a drop in insulation resistance in the small capacitors (group A) during 125°C and 200 V aging were too few to perform a statistical analysis. To precipitate more failures, the applied voltage was increased (higher voltage favors ABD). To compute the values of constants of the Prokopowicz model, failure-terminated tests were planned at three stress levels, 125°C and 285 V, 125°C and 250 V, and 105°C and 285 V. Aging at 125°C and 285 V has been completed and the results are presented in this paper. The time-to-failure of each capacitor was recorded and the mean time to failure (MTTF) at 125°C and 285V aging was calculated using Weibull software. A typical plot of insulation resistance of small capacitors (group A) during 125°C and 285V aging is shown in Fig. 4.

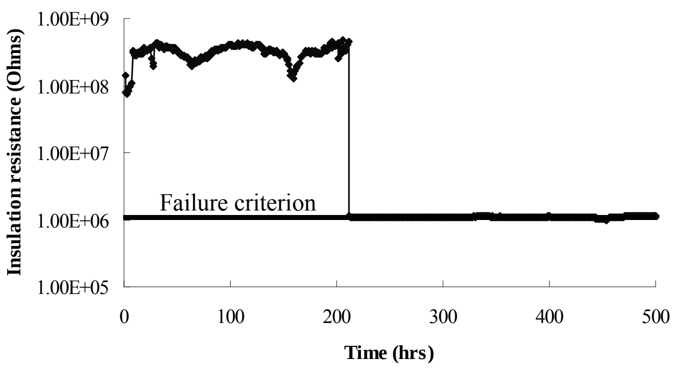

Fig. 4. Insulation resistance of small capacitors (group A) at 125°C and 285 V

It was observed that failures followed two different distributions (termed as "early life" and "wear out" failures), so a mixed Weibull distribution was used as shown in Fig. 5. The parameters of the distribution, MTTF, β (shape parameter), η (scale parameter), and P (cumulative percentage of failure in that distribution) were calculated and are given in Table 1.

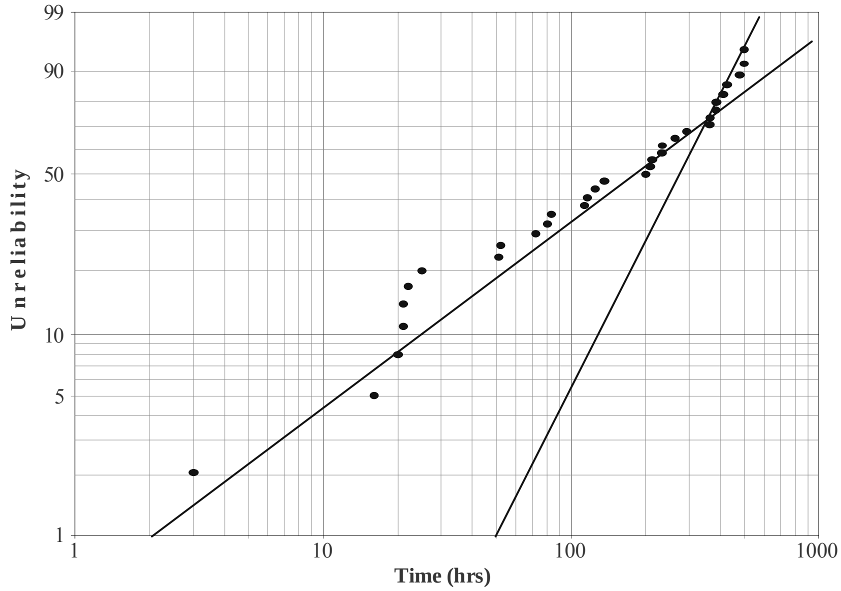

Fig. 5. Unreliability vs. time-to-failure due to IR drop (for group A capacitors) at 125°C and 285 V

Table 1. Statistical analysis of time-to-failure due to IR drop (for group A capacitors) at 125°C and 285 V

Aging condition	Test duration (hrs)	Failed	Survived		MTTF (hrs)	β	η	P
125°C and 285V	500	32	1	Early life	119	1.02	130	0.71
				Wearout	452	5.98	444	0.28

All large capacitors (group B) were found to fail as a result of a sharp drop in insulation resistance within 10 hrs (well below the time-to-failure of small capacitors). The same electric field was experienced by the dielectric of both groups (A and B), so a smaller time-to-failure of large capacitors can be explained by a larger number of defects in the dielectric. The reason for ABD (which is the failure mode in the present study) has been attributed to defects in the dielectric. With an increase in the area of the capacitor the number of defects in the dielectric should increase, which might have led to a shorter time-to-failure for large capacitors (making the assumption of a constant defect density). This implies that the Prokopowicz equation could be modified to include a term which is a function of the capacitor area.

In the temperature and voltage aging test conducted at 125°C and 200 V, no failures were observed due to a decrease in the capacitance [25]. Failures as a result of a decrease in capacitance were observed during aging at 125°C and 285 V. A histogram of the decrease in capacitance is shown in Fig. 6. In some capacitors, the value of capacitance started to fluctuate after failure due to a sharp drop in the insulation resistance. The capacitance data from these capacitors was excluded from the histograms and also from further analysis, since the objective here was to model the behavior of capacitance associated with aging, independently of the behavior of insulation resistance.

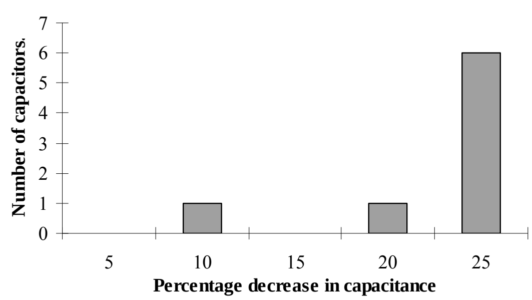

Fig. 6. Decrease in capacitance (for group A capacitors) after 500 hrs at 125°C and 285 V

A typical plot of capacitance during aging for small capacitors is shown in Fig. 7. It was observed that the rate of degradation of capacitance increased rapidly after a particular time, which is referred to as t_o hereafter. Before t_o, the degradation was found to be linear. This changed to logarithmic after t_o. The value of the aging transition time (t_o) was found to be 170.9 ± 5.5

hrs. It implies that there is a change in the capacitance degradation mechanism at this time. The mechanism of degradation before and after t_o is currently under investigation.

$$C = \begin{cases} C_o - mt \,;\, t < t_o \\ C_{o1} - k\ln t \,;\, t > t_o \end{cases} \tag{4}$$

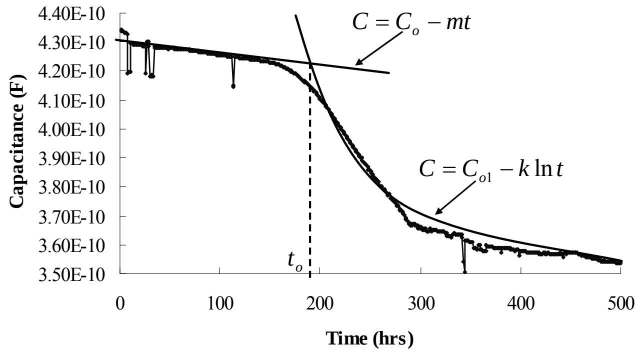

Fig. 7. Typical plot of capacitance (for group A capacitors) at 125°C and 285 V

Linear regression was performed on the capacitance data before and after t_o, and the mean values of the constants (C_o, m, C_{o1}, and k, as defined in Fig. 7) are presented in

Table 2. The value of the regression coefficient (r^2) is also shown in the table. The regression coefficient (r^2) in the linear region was found to be low (0.48) due to frequent drops in the values of capacitance (this might be due to external noise, since the capacitance values were in the picofarad range).

Table 2. Results of regression on the capacitance data (for group A capacitors) at 125°C and 285 V

Aging condition	Linear degradation region			Logarithmic degradation region		
	m	C_o	r^2	k	C_{o1}	r^2
125°C, 285 V	-5.09E-14	4.34E-10	0.48	-7.20E-11	7.84E-10	0.95

Statistical analysis was performed on the time-to-failure data (as a result of a decrease in the capacitance) for small capacitors. A Weibull 3-parameter distribution was fitted to the failure data as shown in Fig. 8, and the parameters of the distribution are given in

Table 3, where γ is the location parameter. The value of time to 50 percent failure (t_{50}) at 125°C and 285 V aging was found to be 392.4 hrs.

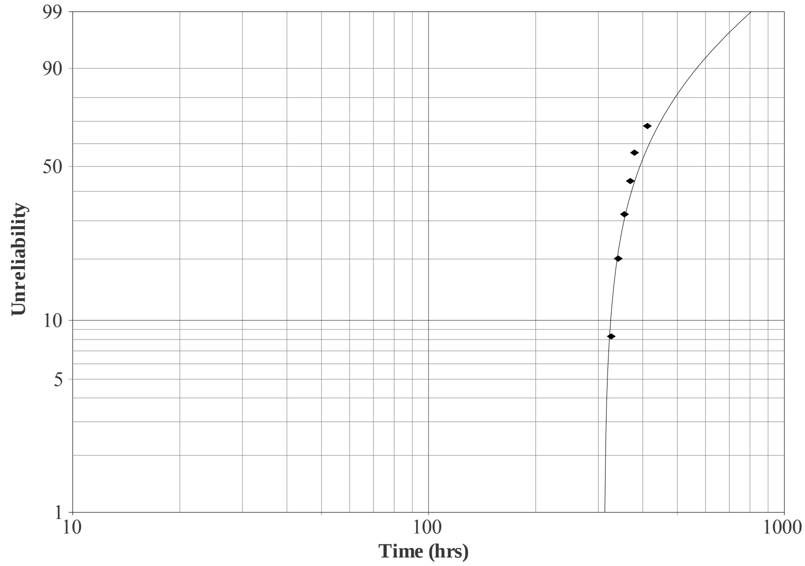

Fig. 8. Unreliability vs. time-to-failure due to capacitance decrease (for group A capacitors) at 125°C and 285 V

Table 3. Statistical analysis of time-to-failure due to capacitance decrease (for group A capacitors)

Aging condition	Test duration (hrs)	Failed	Survived	t_{50} (hrs)	β	η	γ
125°C and 285V	500	6	2	392	1.04	115	312

No failures as a result of decrease in capacitance were observed for large capacitors (group B) at 125°C and 285 V. The degradation in the capacitance for large capacitors was different as compared to small capacitors, and no linear degradation region was found as shown in Fig. 9. The values of constants C_{o1} and k for the logarithmic degradation were found by regression and are presented in
Table 4.

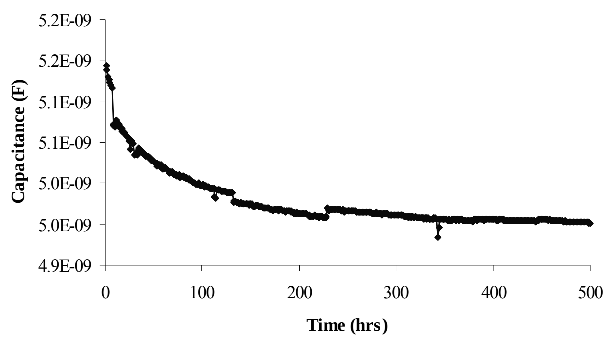

Fig. 9. Typical plot of capacitance (for group B capacitors) at 125°C and 285 V

Table 4. Results of regression on the capacitance data (for group B capacitors) at 125°C and 285 V

Aging condition	Logarithmic degradation region		
	k	C_{o1}	r^2
125°C, 285 V	-4.13E-11	5.10E-9	0.96

The values of the constant k for the logarithmic degradation rate for small and large capacitors are comparable to each other implying that the logarithmic degradation was due to a change in the material properties of the dielectric. The time-to-failure (TTF) as a result of a decrease (20%) in capacitance in the logarithmic degradation region can be computed by:

$$TTF = \ln^{-1}\left(\frac{0.8C_{01}}{k}\right) \tag{5}$$

Since the initial value of capacitance (C_{01}) of large capacitors was around one order of magnitude higher than the capacitance of small capacitors and the value of k was found to be comparable, no failures were observed in large capacitors during the duration of test.

In the future, temperature and voltage tests will be conducted at 125°C, 250V and 105°C, 285V and the values of Prokopowicz constants will be computed. Since failures were also observed as a result of a decrease in capacitance, a model for the TTF (as a result of a decrease in capacitance) will be developed.

6 Temperature-humidity-bias tests

The objective of conducting temperature-humidity-bias tests was to investigate the effects of an applied voltage under elevated temperature and humidity conditions. Three test vehicles were biased at 0, 5, and 150 V in an environmental chamber maintained at 85°C and 85% RH. 36 out of 80 capacitors were selected from group A (small capacitors) and 4 out of 6 capacitors were selected from group B (large capacitors). The parameters of 120 capacitors were monitored in-situ every one hour.

Thus far 395 hours of testing have been completed and the test is still proceeding. No failures were observed in the test vehicle that was biased at 0 and 5 V. At both these stress levels the capacitance was found to increase with time, as expected. Typical plots of the capacitance of group A and group B capacitors (maintained at 85°C and 85% RH) are shown in Fig. 10 and Fig. 11, respectively. It can be observed that for small capacitors (group A) the capacitance stabilized within the first 100 hrs, whereas in large capacitors (group B) the capacitance is still increasing. The reason for this behavior is currently under investigation.

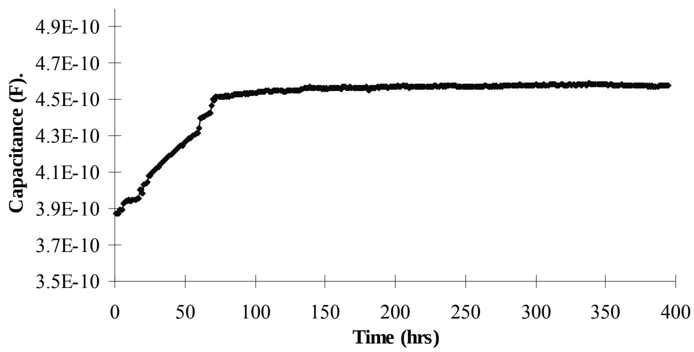

Fig. 10. Capacitance of group A capacitors (maintained at 85°C, 85% RH, and 0 V)

The average increase in capacitance after 395 hrs for group A and group B capacitors maintained at 85°C, 85% RH and 85°C, 85% RH, and 5 V are given in Table 5. The dissipation factor was also found to increase due to moisture absorption in the dielectric.

Table 5. Percentage increase in capacitance

Stress level	Group A	Group B
85°C and 85% RH	17.3 ± 1.7	13.9 ± 0.5
85°C, 85% RH, and 5 V	17.3 ± 1.7	13.8 ± 0.6

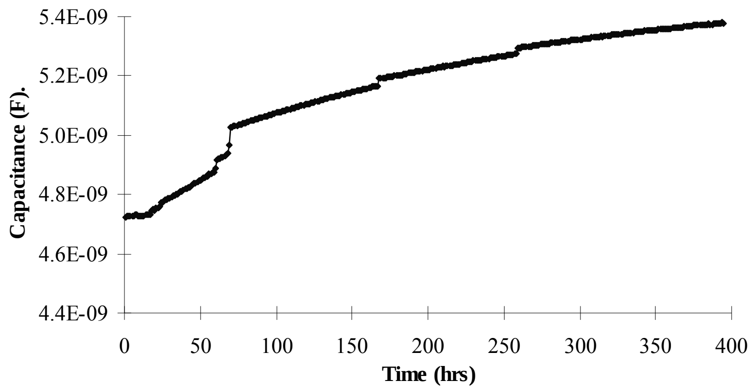

Fig. 11. Capacitance of group B capacitors (maintained at 85^{o}C, 85% RH, and 0 V)

Insulation resistance was found to increase on both test vehicles (that were biased at 0 and 5 V) and is shown in Fig. 12. The reason for this increase in insulation resistance under humid conditions is currently under investigation.

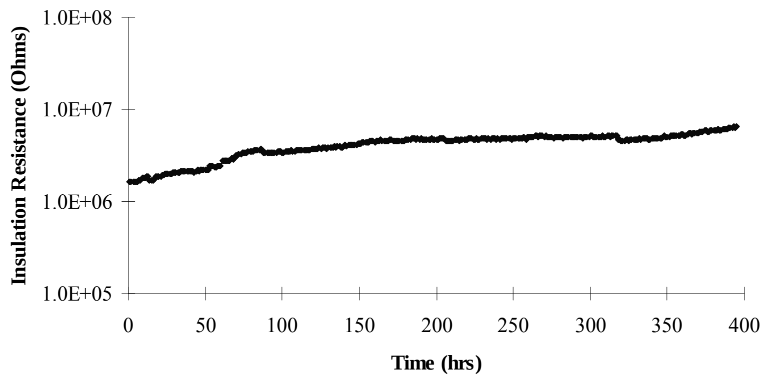

Fig. 12. Insulation resistance of group A capacitors (maintained at 85^{o}C, 85% RH, and 0 V)

Failures were observed due to a sharp drop in insulation resistance on the test vehicle that was biased at 150 V. A typical plot of insulation resistance of a failed capacitor is shown in Fig. 13. Many intermittent failures were observed before the permanent failure. 32 out of 36 capacitors of group A and 4 out of 4 capacitors of group B failed within 395 hrs. The value of capacitance started to fluctuate after failure (as a result of a sharp drop in IR), so the increase in capacitance at this stress level is not calculated. The THB test at 150 V bias will be terminated upon failure of the remaining capacitors of group A.

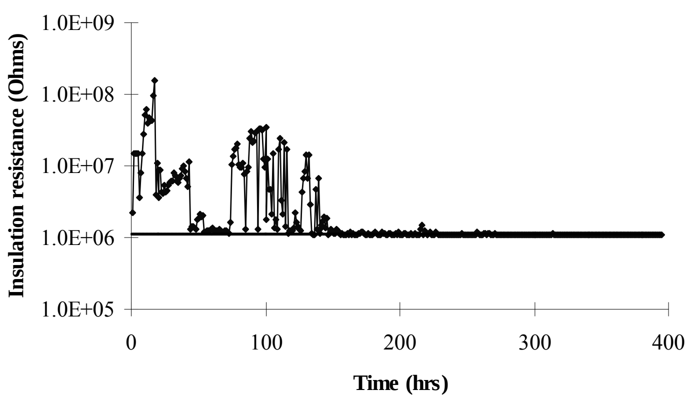

Fig. 13. Insulation resistance of group A capacitors (maintained at 85^{o}C, 85% RH, and 150 V)

The THB test at 0 and 5 V bias will be continued for up to 2500 hrs or complete failure of all capacitors (whichever is earlier). Any differences in the measured parameters of the boards biased at 0 and 5 V will be analyzed.

7 Conclusions

The failure mode of embedded capacitors with an epoxy-barium titanate dielectric during temperature and voltage aging (125^{o}C and 285 V) was found to be a sharp drop in the insulation resistance indicating avalanche breakdown (ABD) and a gradual decrease in capacitance. ABD failures were found to follow two distributions, indicating early life and wearout failures. The MTTFs for early life and wearout life for small capacitors (0.026 in^2 in area) were found to be 119 and 452 hrs, respectively. It was found that the time-to-failure as a result of ABD dropped with an increase in the area of the capacitor due to an increase in the number of defects in the dielectric. The nature of degradation of capacitance during aging (125^{o}C and 285 V) was different for small and large capacitors. The degradation of the small capacitors (0.026 in^2 in area) was found to be linear followed by a logarithmic degradation. Large capacitors (0.19 in^2 in area) had only a logarithmic degradation region. The effect of area on the degradation in capacitance is currently under investigation. The rate of logarithmic degradation for small and large capacitors was similar, implying a change in a material property (possibly dielectric constant) as the reason for logarithmic degradation. The time-to-50% failure (as a result of a decrease in capacitance) for group A capacitors was found to be 392 hrs. No failures as a result of a decrease in a capacitance were observed in group B capacitors, during 500 hrs of aging, since the time-to-failure in the logarithmic degradation region is proportional to the initial value of capacitance (the initial value of capacitance of group B capacitors was about one order of magnitude higher than that of group A capacitors).

Under elevated temperature and humidity conditions (85^{o}C and 85% RH for 395 hrs) the capacitance was found to increase by about 15% for both groups of capacitors due to moisture absorption in the dielectric. The dielectric constant of water (≈78) is greater than the dielectric constant of the composite dielectric (≈16). Dissipation factor was also found to increase due to moisture absorption in the dielectric. The insulation resistance of this dielectric remained stable after 395 hours of testing at 5 V and 85^{o}C and 85% RH. Failures due to a sharp drop in insulation resistance (indicating avalanche breakdown) were observed when the applied bias was 150 V under the same environmental conditions.

Temperature and voltage aging and THB tests will continue and further results will be reported in a future publication. Based on the results, recommendations will be provided regarding the design and stress levels for usage of these devices.

8 Acknowledgements

This research was supported by the members of the CALCE Electronic Products and Systems Consortium at the University of Maryland, College Park. The authors would also like to acknowledge Mark Zimmerman of CALCE for his valuable comments on the paper.

9 References:

[1] A. Madou and L. Martens, “Electrical Behavior of Decoupling Capacitors Embedded in Multilayered PCBs,” IEEE Transactions on Electromagnetic Compatibility, pp. 549-556, Vol. 43, No. 4, 2001.

[2] M. Alam, M. H. Azarian, M. Osterman, and M. Pecht, “Effectiveness of Embedded Capacitors in Reducing the Number of Surface Mount Capacitors for Decoupling Applications,” Circuit World, Vol. 36, Issue 1, 2010 (In Press).

[3] S. Swartz, “Topics in Electronic Ceramics,” IEEE Transactions on Electrical Insulation, pp. 935-987, Vol. 25, No. 5, 1990.

[4] S. Wada, T. Hoshina, H. Yasuno, S. Nam, H. Kakemoto, T. Tsurumi, and M. Yashima, “Size Dependence of Dielectric Properties for nm-Sized Barium Titanate Crystallites and its Origin,” Journal of Korean Physical Society, pp. 303-307, Vol. 46, No. 1, 2005.

[5] K. Jang and K. Paik, “Screen Printable Epoxy/$BaTiO_3$ Embedded Capacitor Pastes with High Dielectric Constant for Organic Substrate Applications,” Journal of Applied Polymer Science, pp. 798-807, Vol. 110, 2008.

[6] K. Paik, J. Hyun, S. Lee, and K. Jang, “Epoxy/$BaTiO_3$ ($SrTiO_3$) Composite Films and Pastes for High Dielectric Constant and Low Tolerance Embedded Capacitors in Organic Substrates,” 1st Electronics Systemintegration Technology Conference, pp. 794-801, Vol. 2, 2006. Dresden, Germany.

[7] J. Xu, K. Moon, P. Pramanik, S. Bhattacharya, and C. Wong, “Optimization of Epoxy-Barium Titanate Nanocomposites for High Performance Embedded Capacitor Components,” IEEE Transactions on Components and Packaging Technologies,” pp. 248-253, Vol. 30, No. 2, 2007.

[8] M. Pecht, L. Nguyen, and E. Hakim, Plastic Encapsulated Microelectronics, John Wiley & Sons, New York, NY, 1994.

[9] W. Mason, “Aging of the Properties of Barium Titanate and Related Ferroelectric Ceramics,” The Journal of the Acoustical Society of America, pp. 73-85, Vol. 27, No. 1, 1955.

[10] D. Donahoe, M. Pecht, I. Lloyd, and S. Ganesan, “Moisture Induced Degradation of Multilayer Ceramic Capacitors,” Microelectronics Reliability, pp. 400-408, Vol. 46, 2006.

[11] L. Mitoseriu, V. Tura, M. Curteanu, D. Popovici, and A. Anghel, “Aging Effects in Pure and Doped Barium Titanate Ceramics,” IEEE Transactions on Dielectrics and Electrical Insulation, pp. 500-506, Vol. 8, No. 3, 2001.

[12] K. Jang and K. Paik, “A Study on Epoxy/$BaTiO_3$ Embedded Capacitor Pastes for Organic Substrates,” Electronic Components and Technology Conference, pp. 1504-1509, 2006, San Diego, CA.

[13] B. Rawal and N. Chan, “Conduction and Failure Mechanisms in Barium Titanate Based Ceramics under Highly Accelerated Conditions,” AVX Technical Report, Myrtle Beach, SC.

[14] H. Lee and L. Burton,” Charge Carriers and Time Dependent Currents in $BaTiO_3$-Based Ceramic,” IEEE Transactions on Components, Hybrids, and Manufacturing Technology, pp. 469-474, Vol. CHMT-9, No.4, 1986.

[15] J. Yamamatsu, N. Kawano, T. Arashi, A. Sato, Y. Nakano, and T. Nomura, “Reliability of Multilayer Ceramic Capacitors with Nickel Electrodes,” Journal of Power Sources, pp. 199-203, Vol. 60, 1996.

[16] T. Prokopowicz and A. Vaskas, “Research and Development, Intrinsic Reliability, Subminiature Ceramic Capacitors,” Final Report, ECOM-90705-F, pp. 175, NTIS AD-864068, 1969.

[17] W. Minford, “Accelerated Life Testing and Reliability of High K Multilayer Ceramic Capacitors,” IEEE Transactions on Components, Hybrids, and Manufacturing Technology, pp. 297-300, Vol. Chmt-5, No. 3, 1982.

[18] I. Yoo, L. Burton, and F. Stephenson, “Electrical Conduction Mechanisms of Barium-Titanate-Based Thick-Film Capacitors,” IEEE Transactions on Components, Hybrids, and Manufacturing Technology, pp. 274-282, Vol. CHMT-10, No. 2, 1987.

[19] J. Paulsen and E. Reed, “Highly Accelerated Life Testing of Base-Metal-Electrode Ceramic Chip Capacitors,” Microelectronics Reliability, pp. 815-520, Vol. 42, 2002.

[20] G. Maher, T. Prokopowicz, and V. Bheemineni, “High Volumetric Low Fired X7R MLC Capacitor,” 43rd Proceedings of Electronics Components and Technology Conference, pp. 280-284, Orlando, FL, 1993.

[21] M. Randall, A. Gaurav, D. Skamser, and J. Beeson, “Lifetime Modeling of Sub 2 Micron Dielectric Thickness BME MLCC,” Proceedings of Capacitor and Resistor Technology Symposium, pp. 1-7, Scottsdale, AZ, 2003.

[22] R. Das, J. Lauffer, and V. Markovich, “Fabrication, Integration and Reliability of Nanocomposite Bases Embedded Capacitors in Microelectronics Packaging,” Journal of Materials Chemistry, pp. 537-544, Vol. 18, 2008.

[23] S. Lee, J. Hyun, J. Pak, H. Lee, H. Jeon, and K. Paik, “Fabrication and Characterization of Embedded Capacitors in Printed Circuit Boards Using B-Stage Epoxy/$BaTiO_3$ Composite Embedded Capacitor Films (ECFs),” Electronic Components and Technology Conference, pp. 742-746, Lake Buena Vista, Florida, USA, 2008.

[24] C. Zou, J. Fothergill, and S. Rowe, “The Effect of Water Absorption on the Dielectric Properties of Epoxy Nanocomposites,” IEEE Transactions on Dielectrics and Electrical Insulation, pp. 106-117, Vol. 15, No. 1, 2008.

[25] M. Alam, M. H. Azarian, M. Osterman, and M. Pecht, “Reliability of Embedded Planar Capacitors under Temperature and Voltage Stress,” Proceedings of Capacitor and Resistor Technology Symposium, Jacksonville, FL, USA, 2009.

Effect of Environmental Stress and Bias Conditions on Reliability of Embedded Planar Capacitors

Mohammed A. Alam, Michael H. Azarian, Michael Osterman, and Michael Pecht.

Center for Advanced Life Cycle Engineering (CALCE)
University of Maryland
College Park, MD 20742
www.calce.umd.edu

Email: mazarian@calce.umd.edu
Tel: (301) 405-5323

Embedded Planar Capacitor Laminates

- Embedded planar capacitors are thin laminates embedded inside a PWB that serve both as a power/ground plane and as a parallel plate capacitor, and are used in decoupling.
- These laminates consist of a thin dielectric (8-50 μm thick), sandwiched between two copper layers. They enable a reduction in the number of surface mount capacitors[1].

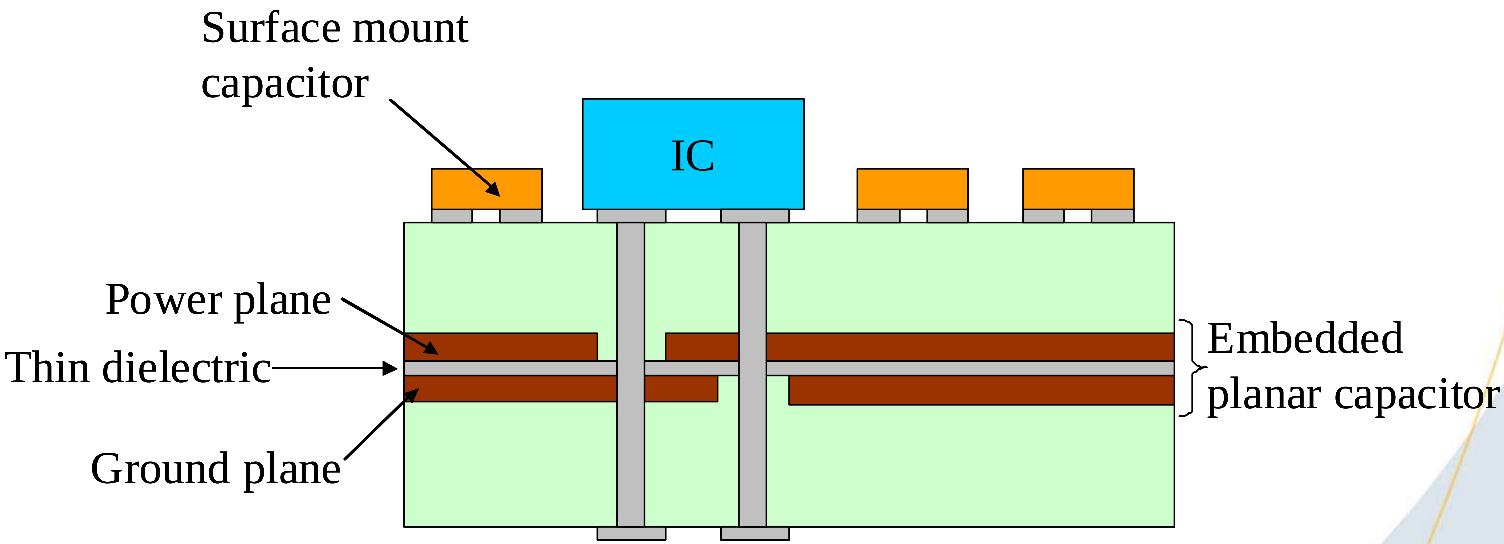

[1]Alam, et al., *Circuit World*, Vol. 36, Issue 1, 2010 (In Press).

Reliability of Embedded Planar Capacitors

- Reliability of embedded capacitors will determine the breadth and success of their practical application.
- The objective of this study is to investigate the effect of
  - **temperature and voltage aging**, and
  - **temperature-humidity-bias**

  on reliability of embedded planar capacitors.
- An epoxy - barium titanate ($BaTiO_3$) composite dielectric is investigated in this study.

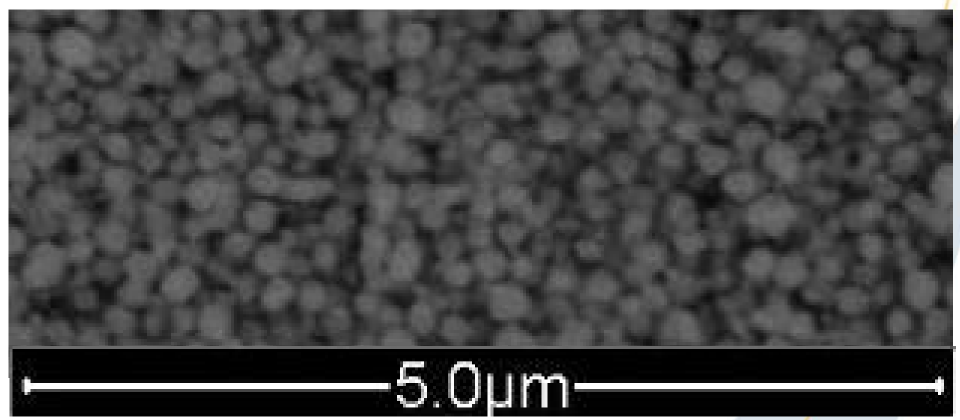

Effect of Temperature:
Reduction in Capacitance

An increase in plate spacing as a result of thermo-mechanical stress generated due to CTE mismatch[1]

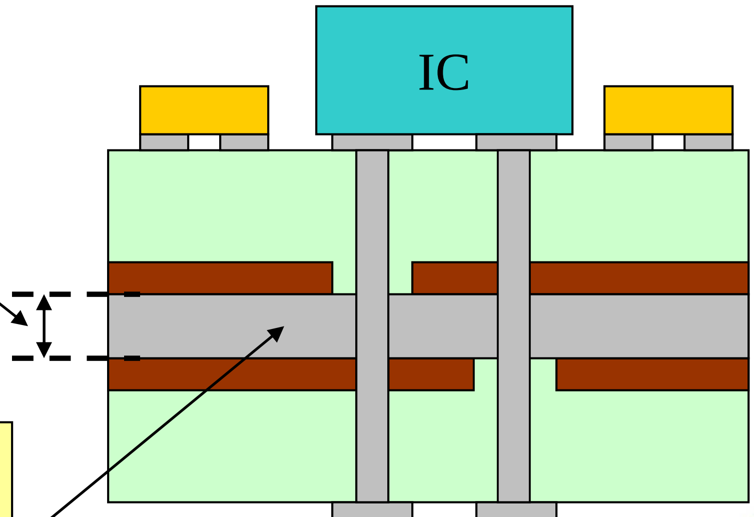

Decrease in the dielectric constant:

- Aging[2] in $BaTiO_3$
- Residual stress relaxation[3] in polymer

[1]Pecht, et al., *Plastic Encapsulated Microelectronics*, John Wiley & Sons, New York, NY, 1994.
[2]Mason, *Journal of the Acoustical Society of America*, pp. 73-85, Vol. 27, No. 1, 1955.
[3]Jang and Paik, ECTC, pp. 1504-1509, 2006, San Diego, CA.

Effect of Temperature and Voltage:
Degradation in Insulation Resistance

- Two failure modes involving degradation in insulation resistance (IR) have been observed[1] in pure $BaTiO_3$:
  - gradual decrease in insulation resistance (**thermal runaway**), which has been attributed to migration of oxygen vacancies;[2]
  - sharp drop in insulation resistance (**avalanche breakdown**), which has been attributed to defects (pores, voids, contamination, etc.) in the dielectric.

[1]Rawal and Chan, "Conduction and Failure Mechanisms in Barium Titanate Based Ceramics under Highly Accelerated Conditions," AVX Technical Report, Myrtle Beach, SC.

[2]Lee and Burton, *IEEE Trans. CHMT*, pp. 469-474, Vol. CHMT-9, No.4, 1986.

Effect of Temperature and Voltage:
Model for IR Degradation

Prokopowicz[1] proposed a model that is used in accelerated life testing of multilayer ceramic capacitors (MLCCs) to precipitate defects in the dielectric.

$$\frac{t_1}{t_2} = \left(\frac{V_2}{V_1}\right)^n \exp\left(\frac{E_a}{k}\left(\frac{1}{T_1} - \frac{1}{T_2}\right)\right)$$

The values of n and E_a for $BaTiO_3$ are reported in literature[1,2]

The values of n and E_a for epoxy-$BaTiO_3$ composite ??

(t is the time-to-failure, V is the voltage, n is the voltage exponent, E_a is the activation energy, k is the Boltzmann constant, T is the temperature, and the subscripts *1* and *2* refer to the two aging conditions.)

[1]Prokopowicz and Vaskas, Final Report, ECOM-90705-F, pp. 175, NTIS AD-864068, 1969.

[2]Rawal and Chan, AVX Technical Report, Myrtle Beach, SC.

Effect of Temperature and Humidity:
Increase in Capacitance

- Moisture absorption leads to an increase[1,2] in the dielectric constant of epoxy-$BaTiO_3$ composites.
- The primary site[3] of absorbed moisture is the interface between the ceramic particle and the polymer matrix.

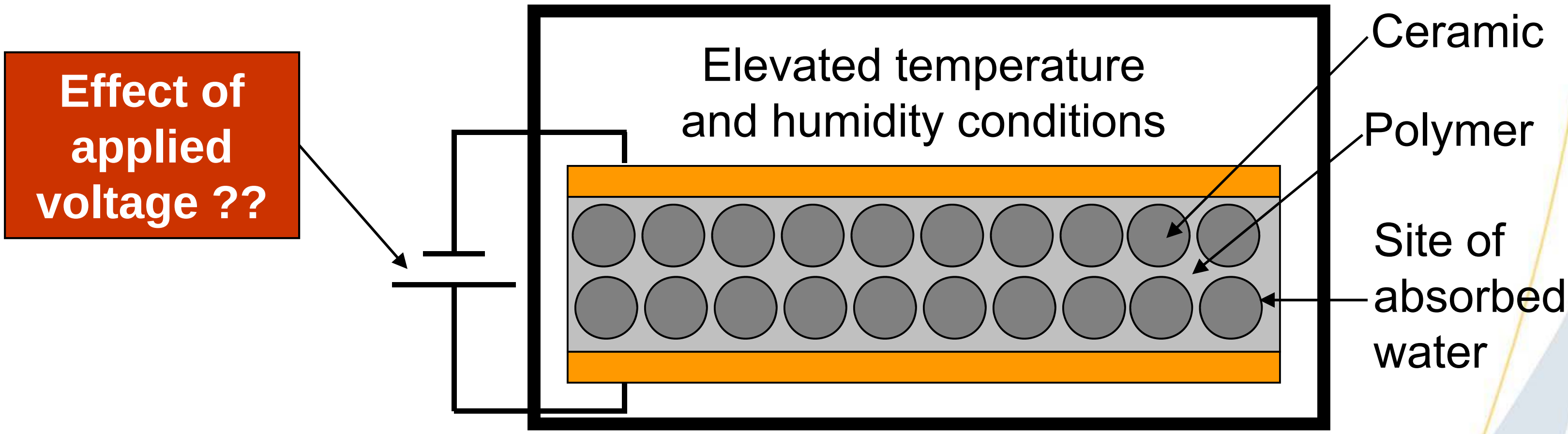

[1]Das, et al., *J. of Materials Chemistry*, pp. 537-544, Vol. 18, 2008.

[2]Lee, et al., ECTC, pp. 742-746, Lake Buena Vista, Florida, 2008.

[3]Zou, et al., *IEEE Trans. on Dielectrics and Electrical Insulation*, pp. 106-117, Vol. 15, No. 1, 2008.

Test Vehicle

- The test vehicle was a 4-layer PWB in which the planar capacitor laminate formed layer 2 (power plane) and layer 3 (ground plane).
- The power plane was etched at various locations to form discrete capacitors.
  The ground plane was continuous.
- Two types of capacitors were investigated:
  - **Group A:** 0.026 in^2, ≈400 pF: 80 capacitors/test vehicle
  - **Group B:** 0.19 in^2, ≈5 nF: 6 capacitors/test vehicle.

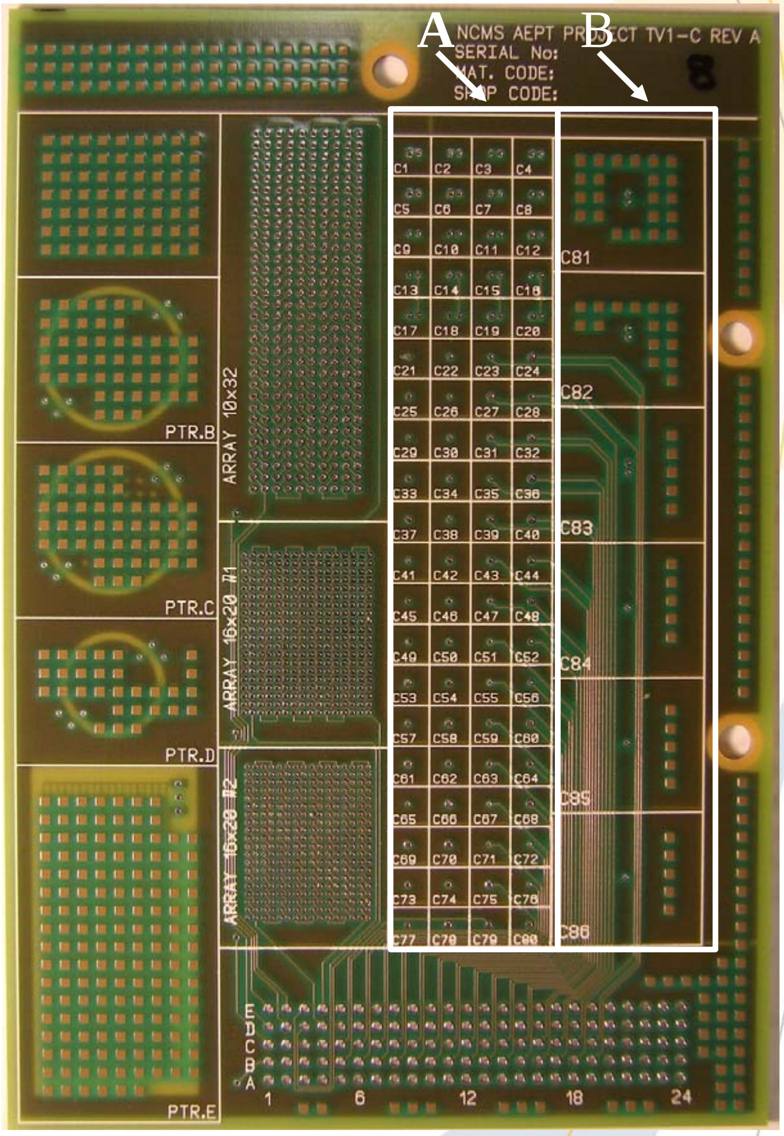

Sectional View of an Embedded Capacitor

- Each capacitor had its power plane connected to a PTH. The ground plane was common to all capacitors.
- The dielectric (8 μm thick) was a composite of $BaTiO_3$ particles, of 250 nm mean diameter, loaded 45% by volume in epoxy.

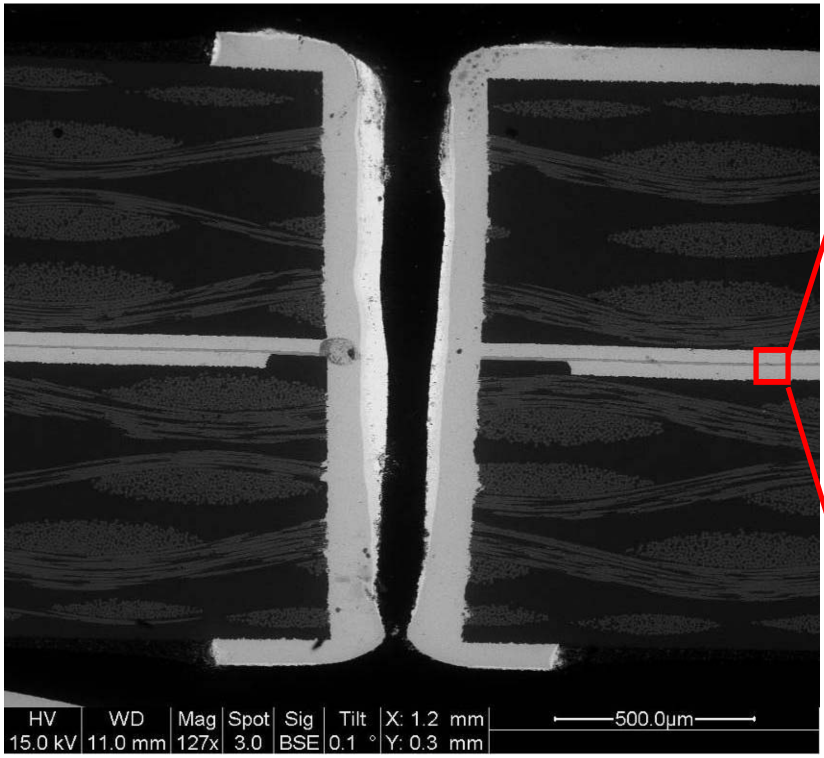

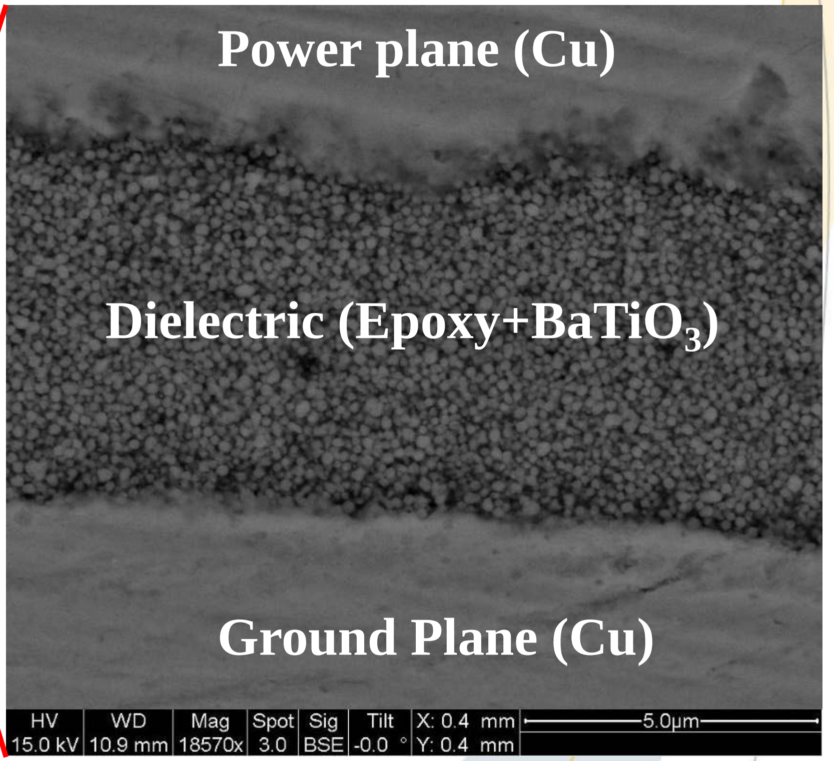

Experimental Setup for Temperature and Voltage Aging

- The parameters of 33 (out of 80) capacitors of group A (small) and 4 (out of 6) capacitors of group B (large) were measured in-situ once every hour:
  - capacitance and dissipation factor were measured at 100 KHz using an LCR meter
  - insulation resistance of the dielectric was measured at 10 V using a high resistance meter.
- In order to limit the current through a capacitor (in case of a dielectric failure), a 1.1 MΩ resistor was placed in series with each capacitor.
- The failure criteria selected were:
  - decrease in capacitance by 20%;
  - increase in dissipation factor by a factor of 2; or
  - decrease in insulation resistance to 1.1 MΩ.

Schematic of the Setup

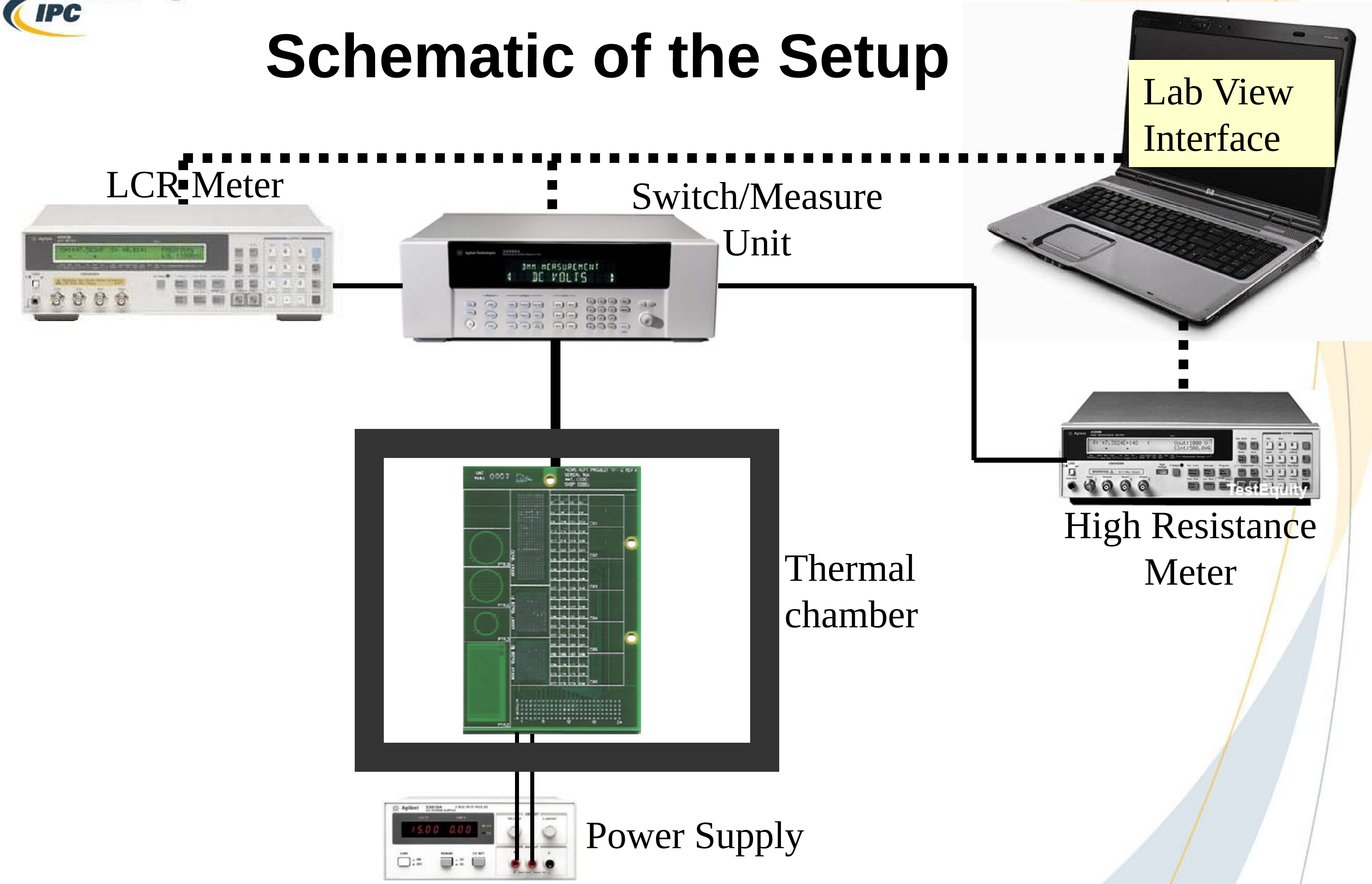

Temperature and Voltage Aging

125^{o}C, 200 V

- **The objective of temperature and voltage aging was to compute the values of constants for Prokopowicz model.**
- A preliminary time-terminated test was conducted by stressing the test vehicle at 125^{o}C and 200 V for 1000 hrs.
- No failures were observed due to a decrease in capacitance.
- Failures were only observed due to a sharp drop in insulation resistance (indicating avalanche breakdown) in:
  - 5 out of 33 capacitors of group A (smaller size), and
  - 4 out of 4 capacitors of group B (larger size).

Test Matrix for Computation of Prokopowicz Model Constants

- Increase the voltage (that favors avalanche breakdown) to precipitate more failures. (200V was too low)
- Experiments were planned at the following stress levels:
  - **125^{o}C and 285 V (this test has been completed)**
  - 125^{o}C and 250 V
  - 105^{o}C and 285 V

Temperature and Voltage Aging

$125^{o}C$, 285 V

- The duration of this test was 500 hrs and failures were observed as a result of:
  - sharp drop in insulation resistance in:
    - 32 out of 33 capacitors of group A (smaller size)
    - 4 out of 4 capacitors of group B* (larger size)
  - gradual decrease in capacitance in:
    - 6 out of 33 capacitors of group A
    - 0 out of 4 capacitors of group B
- The mean time-to-failure (MTTF) as a result of the above failure modes was calculated using Weibull statistics.

*Due to a small sample size, Weibull analysis was not performed on group B capacitors.

Behavior of Insulation Resistance

125°C, 285 V in Group A Capacitors

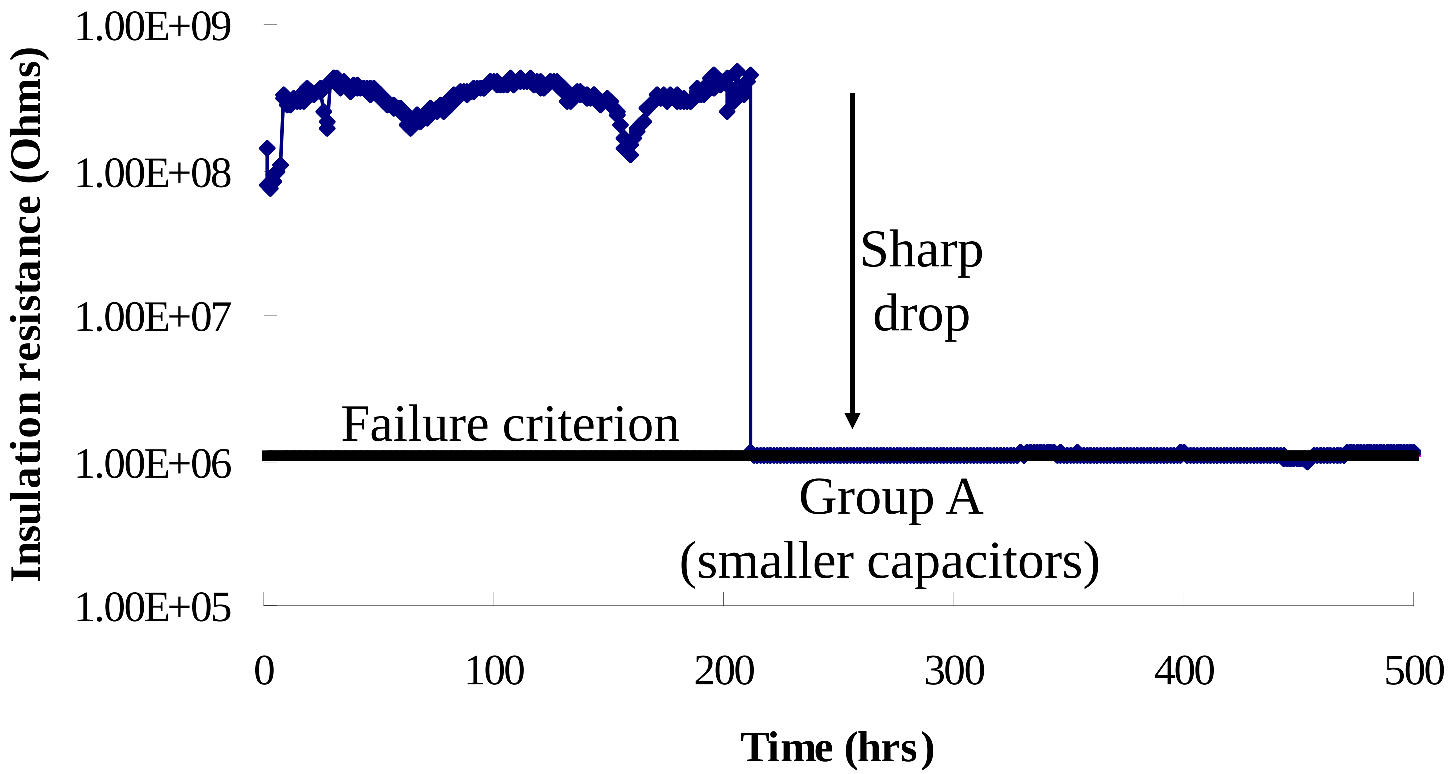

- Capacitors of group B (larger) showed similar drops in insulation resistance but all of them failed within 10 hrs.
- **A shorter time-to-failure of group B capacitors can be explained by a larger number of defects in the dielectric.**

Weibull Analysis

(Sharp drop in insulation resistance in group A at 125°C, 285 V)

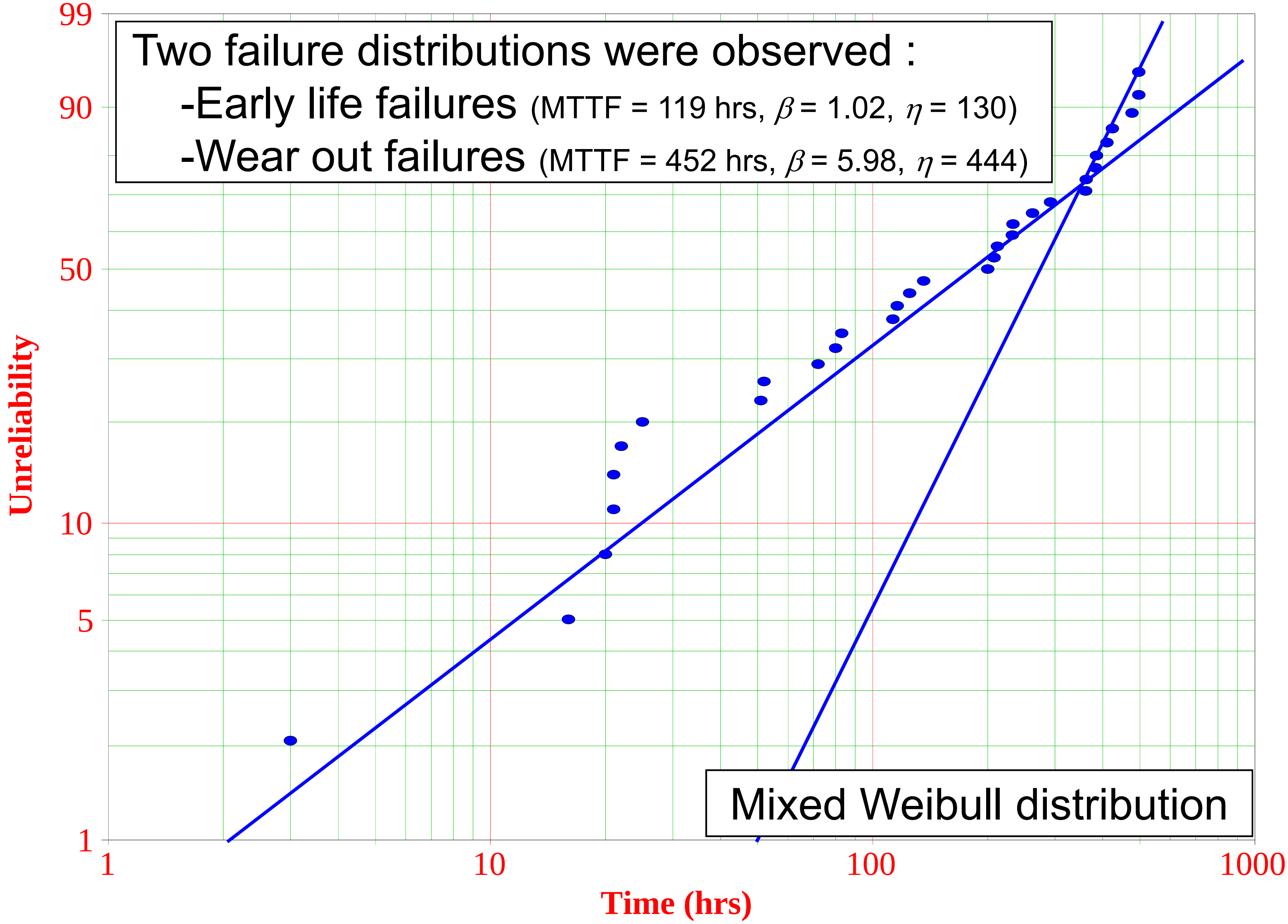

Behavior of Capacitance

(at 125ºC, 285 V in Group A Capacitors)

It was observed that the rate of degradation of capacitance increased rapidly after a particular time, t_o, which is referred to as the aging transition time.

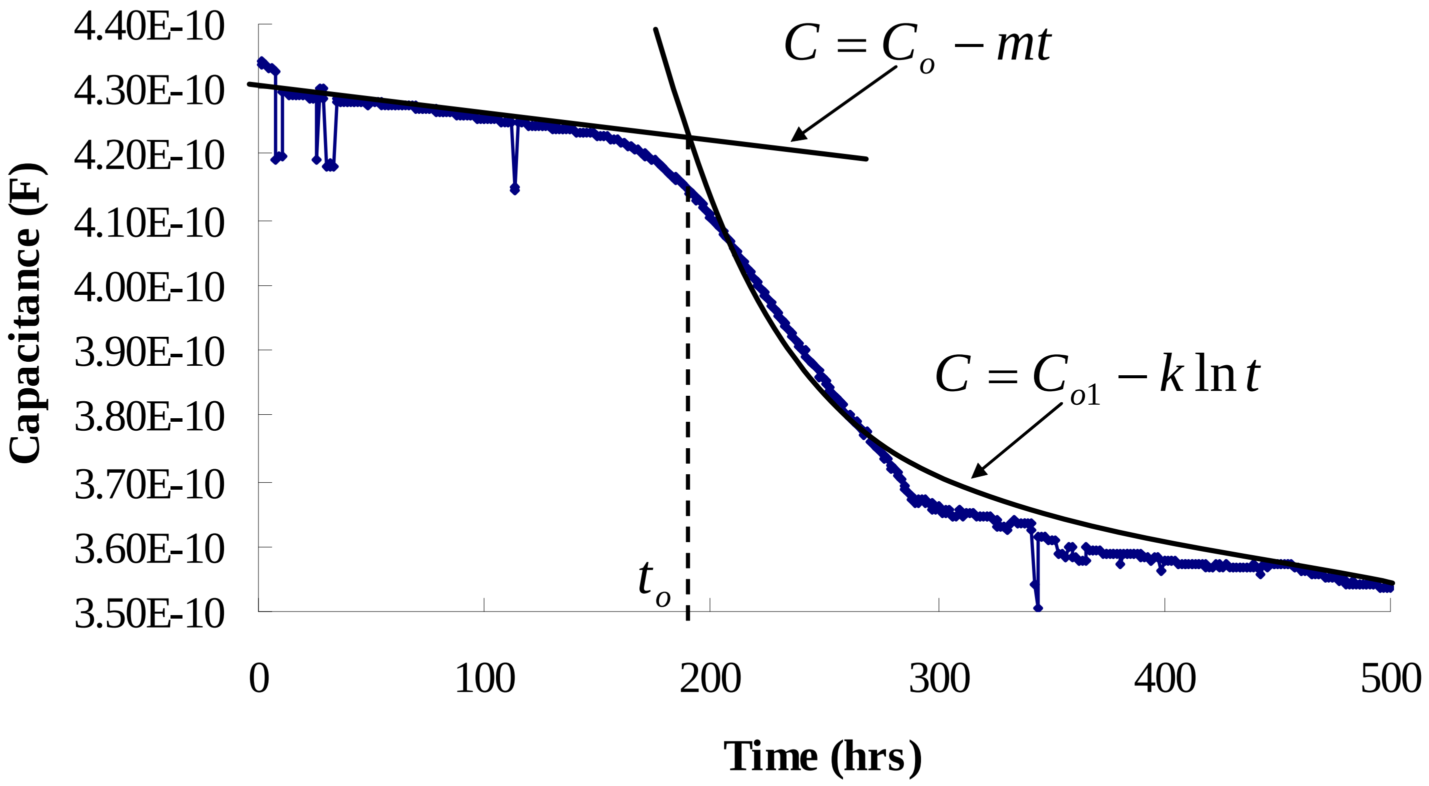

Decrease in Capacitance

(at 125^{o}C, 285 V in Group A Capacitors)

- In some capacitors, the value of capacitance started to fluctuate after failure due to a sharp drop in the insulation resistance.
- Data of such capacitors are eliminated from further analysis since the objective was to model the behavior of capacitance as a result of aging (independently of the behavior of IR).

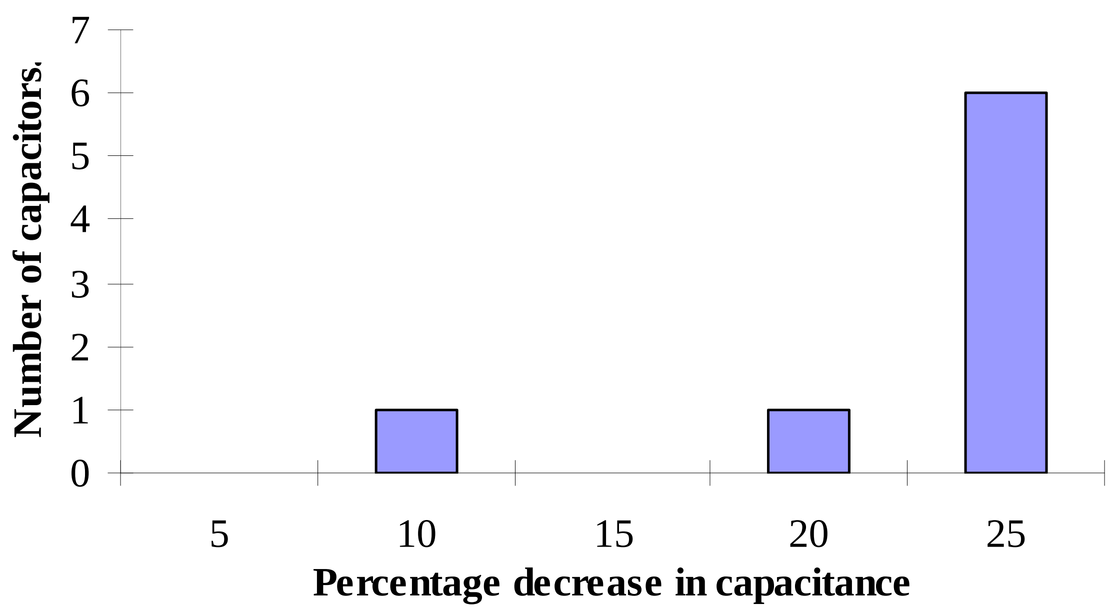

Weibull Analysis

(Gradual decrease in capacitance in group A at 125^{o}C, 285 V)

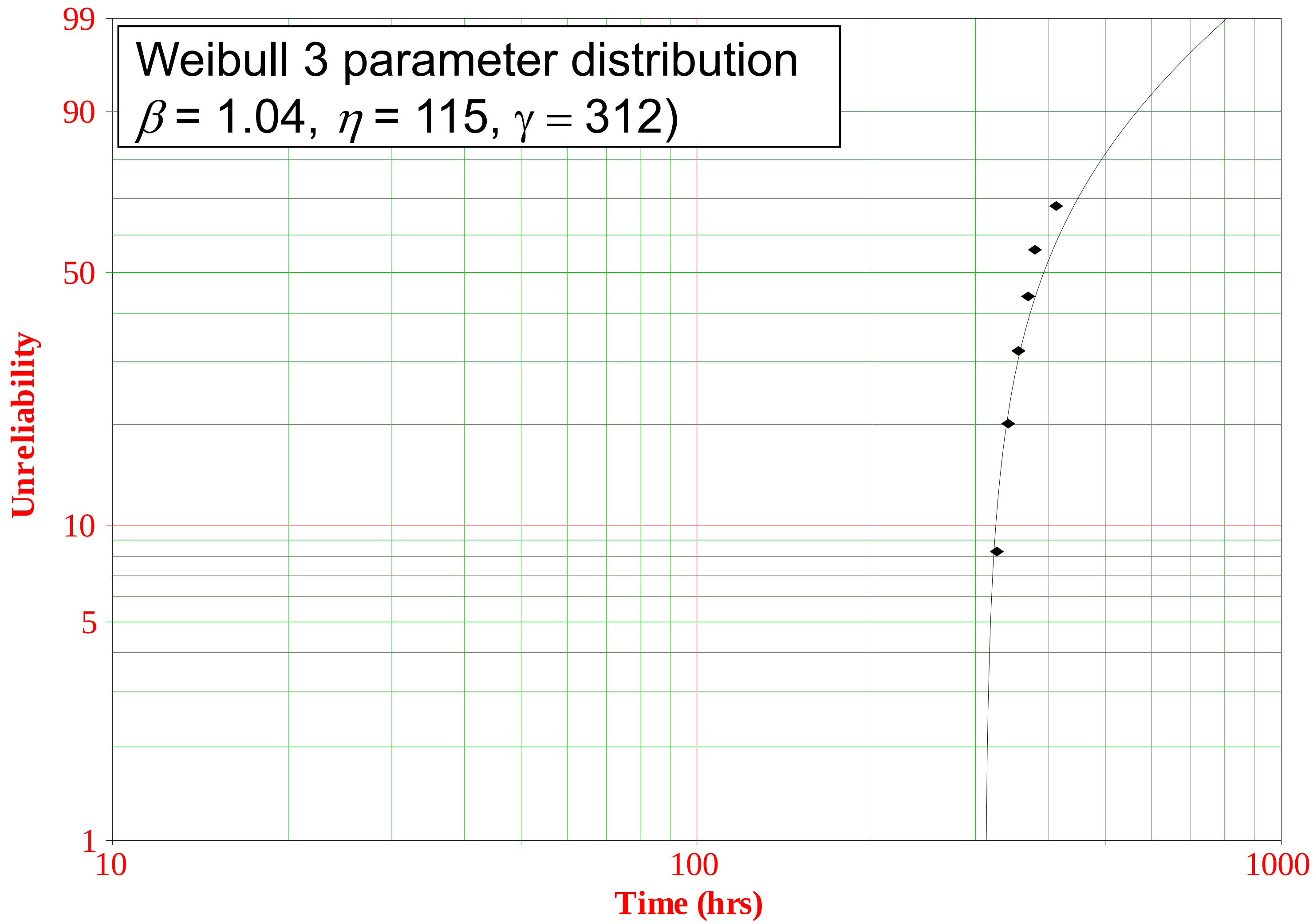

Behavior of Capacitance

(at 125^{o}C, 285 V in Group B Capacitors)

- **Failures were not observed in group B (large) capacitors due to a large value of initial capacitance (C_{o1}) as compared to group A.**
- The linear degradation region in capacitance was absent in group B capacitors (t_o=0).

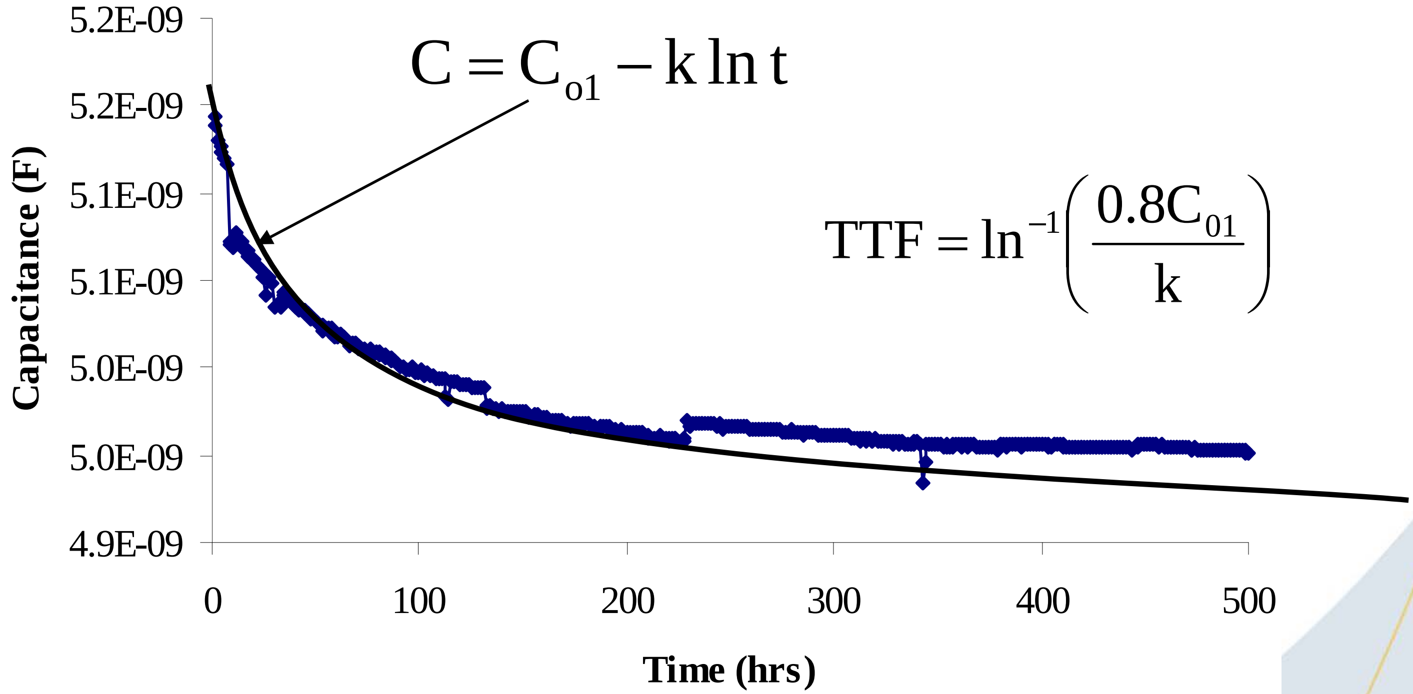

Regression on Capacitance Data

(at 125^{o}C, 285 V in Group A and B Capacitors)

- Regression was performed on the capacitance data to obtain the values of C_o, m, C_{o1}, and k, whose mean values are presented below.

	Aging condition	Linear degradation			Logarithmic degradation		
		m	C_o	r^2	k	C_{o1}	r^2
Group A	125^{o}C, 285 V	-5.1×10^{-14}	4.3×10^{-10}	0.48	-7.2×10^{-11}	7.8×10^{-10}	0.95
Group B					-4.1×10^{-11}	5.1×10^{-9}	0.96

- The values of k for group A and B capacitors are similar, implying similar degradation mechanisms in the logarithmic degradation region.
- **The differences in the behavior of small and large capacitors is currently under investigation.**

Temperature-Humidity-Bias Tests

- Three test vehicles were biased at:
  - 0 V,
  - 5 V, and
  - 150 V,

  in an environmental chamber maintained at 85^{o}C and 85% RH.
- 36 out of 80 capacitors were tested from group A (small capacitors) and 4 out of 6 capacitors were tested from group B (large capacitors).
- The following parameters of all 120 [(36+4)$\times$3] capacitors were monitored once every hour:
  - Capacitance (at 100 KHz using LCR meter),
  - Dissipation factor (at 100 KHz using LCR meter), and
  - Insulation resistance (at 10 V using high resistance meter).

Setup for THB tests

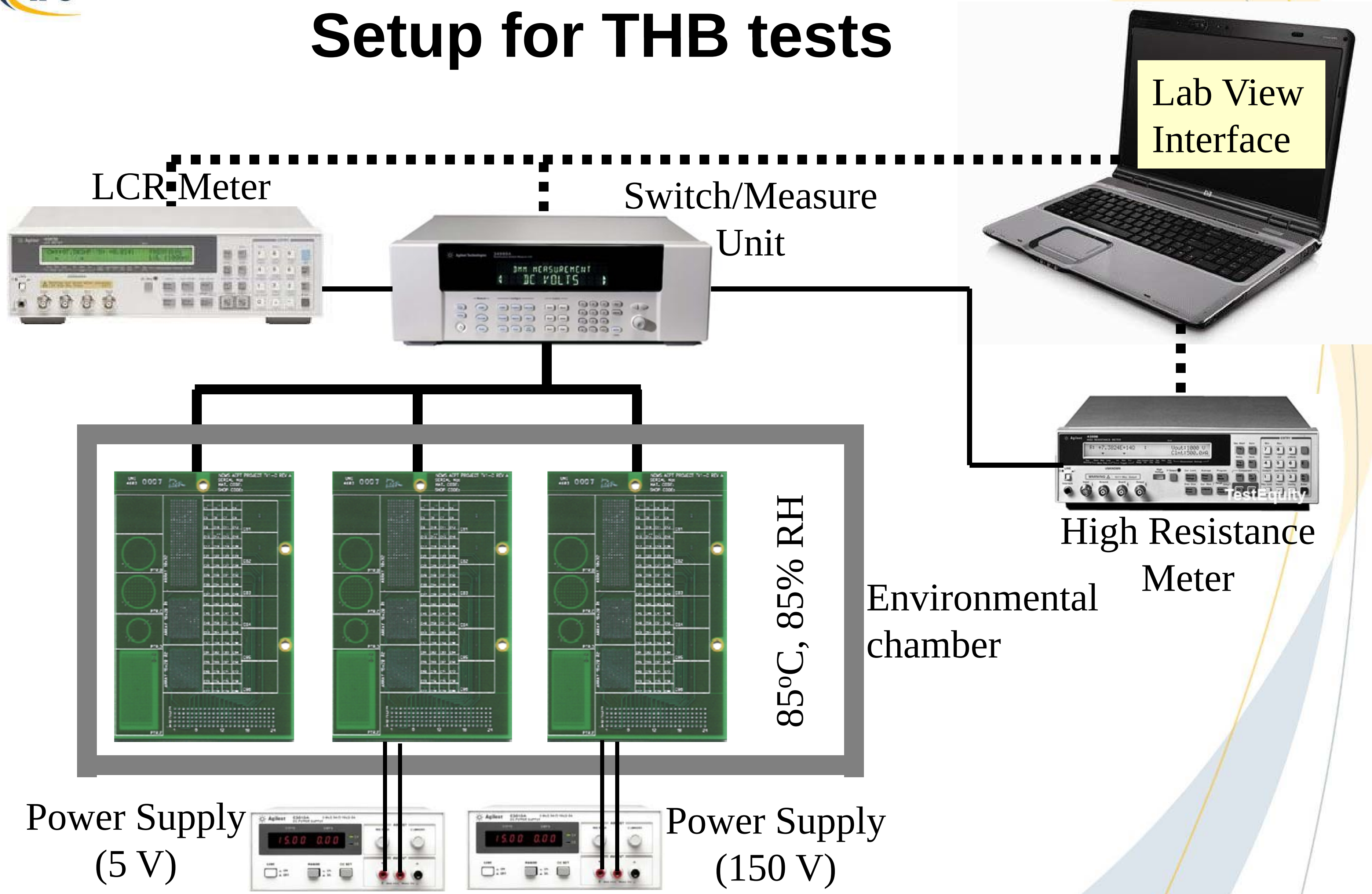

Results of THB Tests

- 395 hrs of test has been completed and the capacitance was found to increase at all stress levels.
- The average increase in capacitance after 395 hrs at 85^{o}C, 85% RH, and 0 V was:
  - 17.3 $\pm$ 1.7 % for small capacitors (group A: smaller)
  - 13.9 $\pm$ 0.5 % for large capacitors (group B: larger).
- The average increase in capacitance after 395 hrs at 85^{o}C, 85%, RH and 5 V was:
  - 12.3 $\pm$ 1.9 % for small capacitors (group A)
  - 13.8 $\pm$ 0.6 % for large capacitors (group B).
- Failures as a result of a sharp drop in insulation resistance were only observed at 85^{o}C, 85%, RH and 150 V.

Behavior of Capacitance

(For Group A capacitors at 85^{o}C, 85% RH, and 0 V)

- **In group A (small) capacitors the capacitance increased within first 100 hrs and then stabilized.**
- Similar behavior was observed for the test vehicle biased at 5 V.

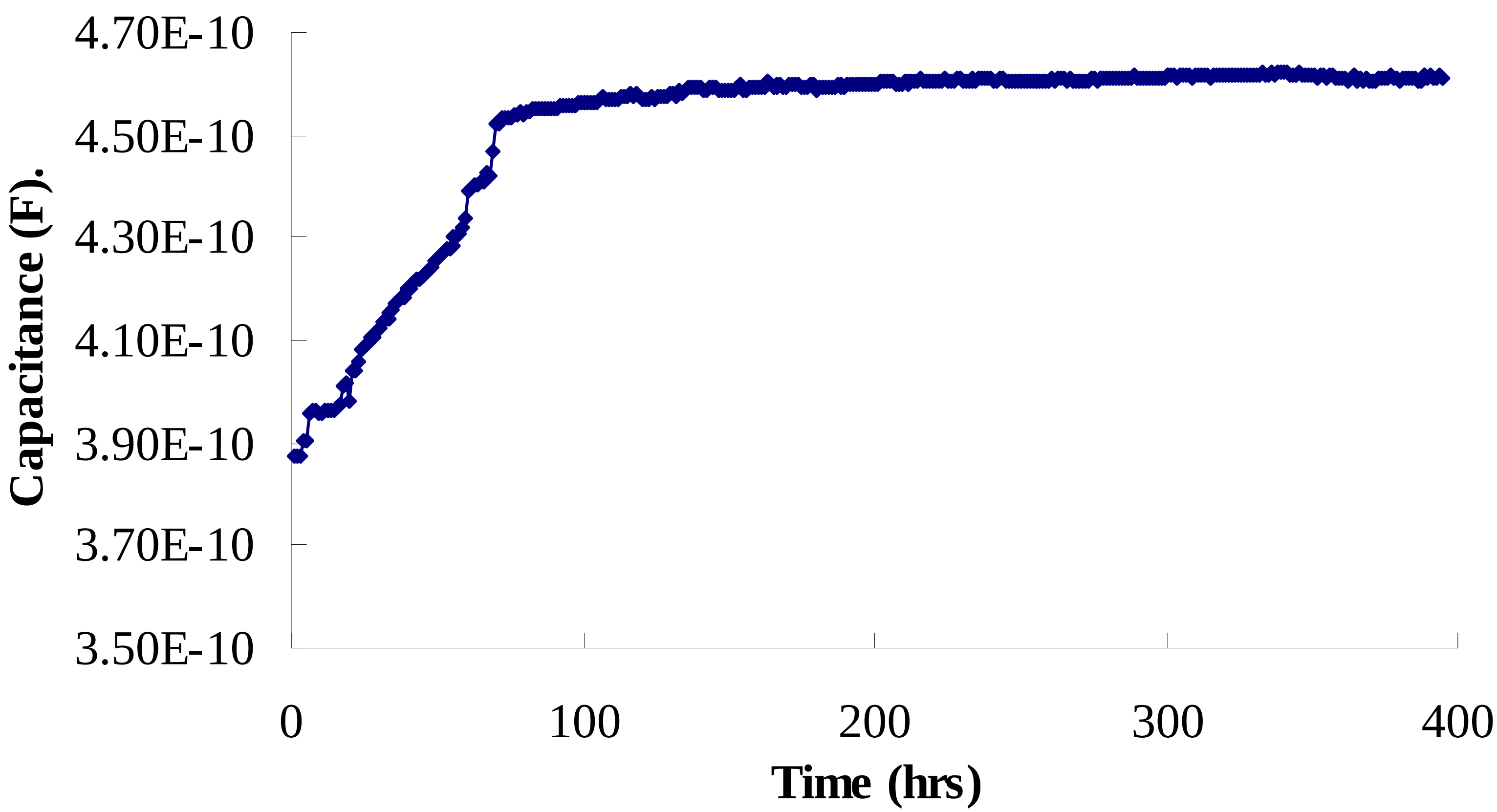

Behavior of Capacitance

(For Group B capacitors at 85^{o}C, 85% RH, and 0 V)

- **In group B (large) capacitors the increase in the capacitance is not observed to achieve a steady state value in 395 hrs.**
- Similar behavior was observed for the test vehicle biased at 5 V.

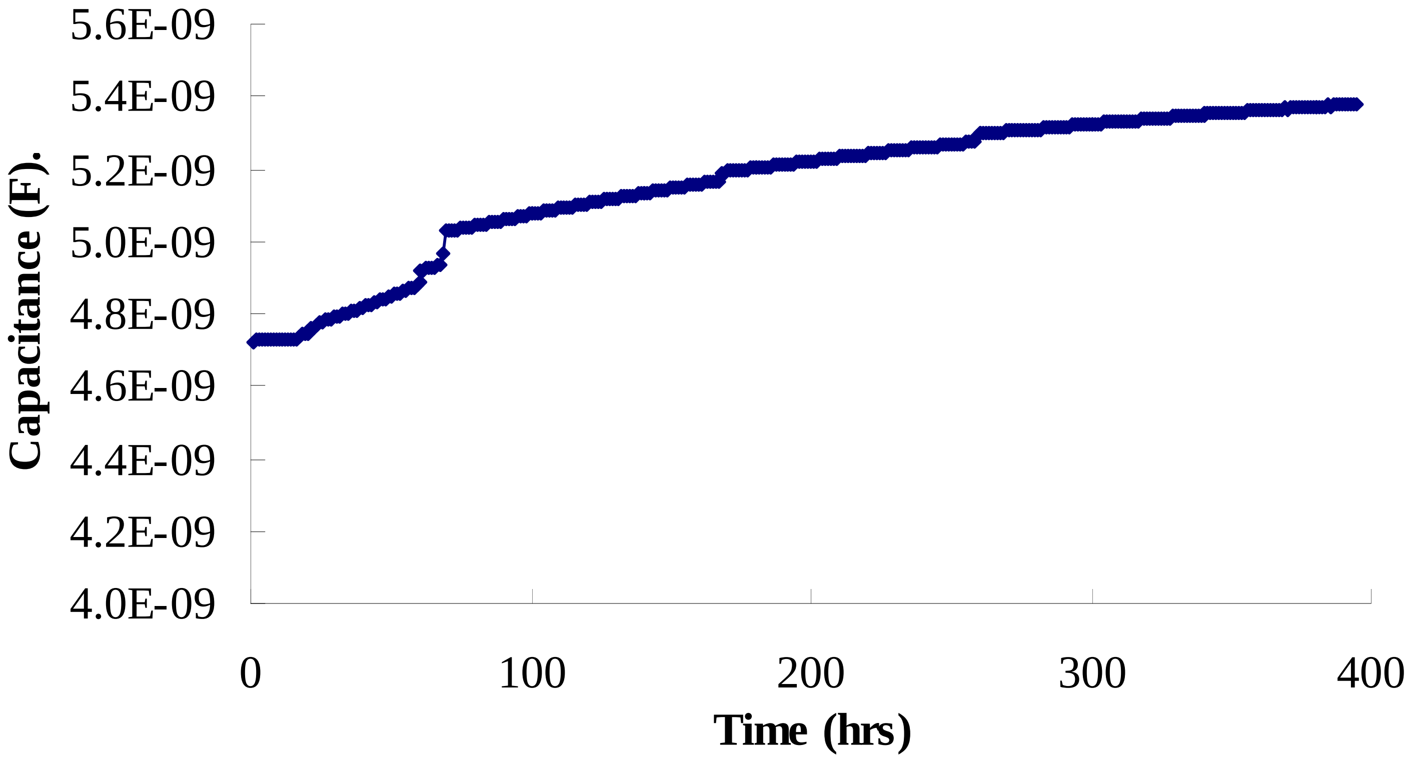

Behavior of Insulation Resistance

(For Group A capacitors at 85^{o}C, 85% RH, and 0 V)

- Insulation resistance was found to increase with time at both 0 V bias and 5 V bias.
- The increase in the insulation resistance under humid conditions is currently under investigation.

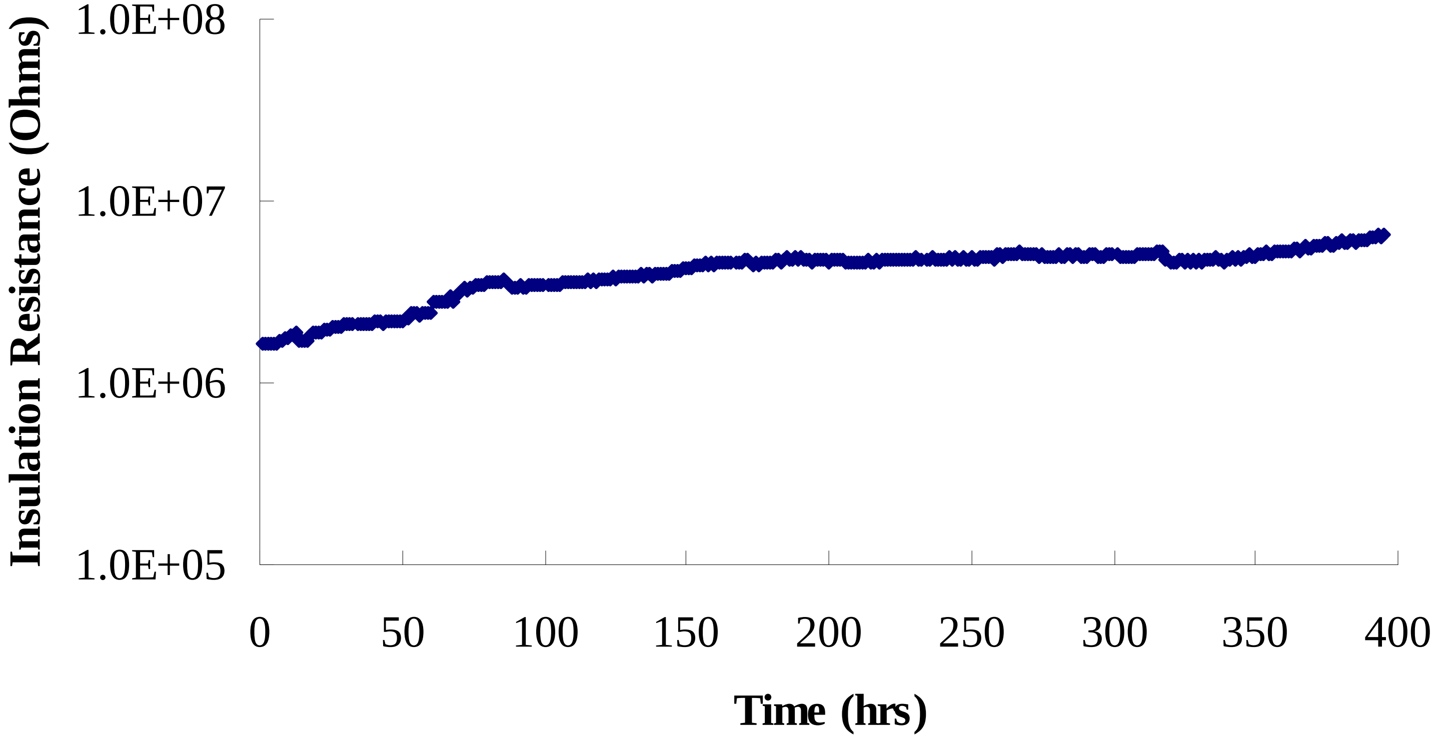

Behavior of Insulation Resistance

(For Group A capacitors at 85^{o}C, 85% RH, and 150V)

Failures were observed due to a sharp drop in insulation resistance at 150 V, and

- 32 out of 36 capacitors of group A, and
- 4 out of 4 capacitors of group B

failed in 395 hrs.

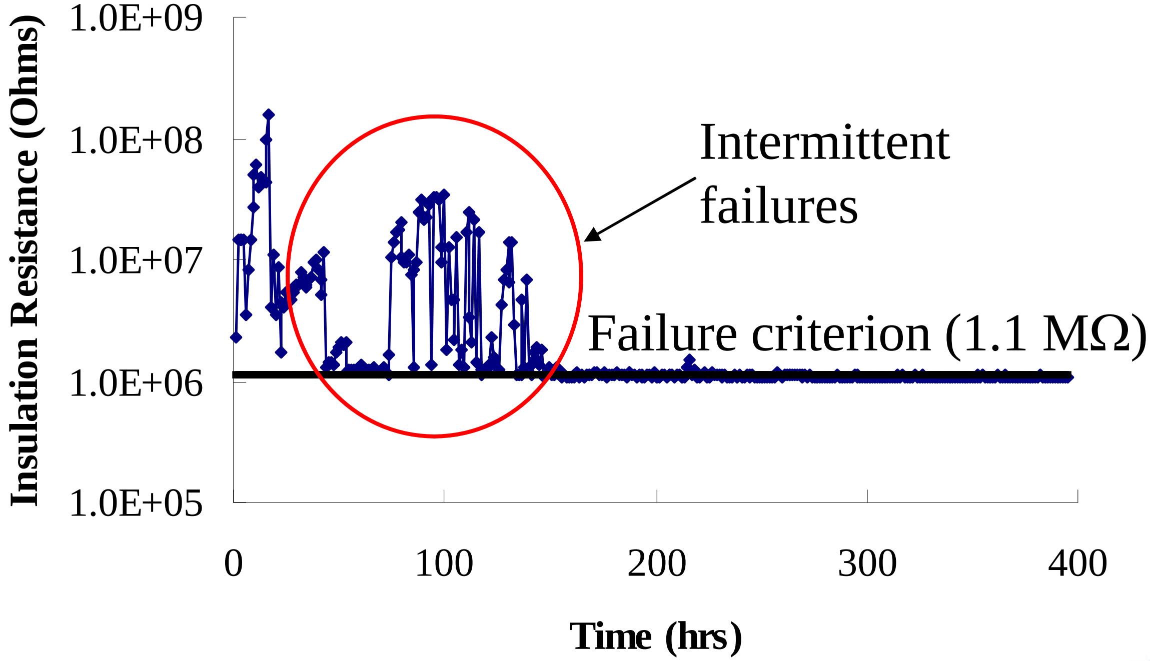

Conclusions

Temperature and voltage aging (125^{o}C, 285 V for 500 hrs):

- The failure mode of these embedded capacitors was found to be a:
  - sharp drop in insulation resistance (avalanche breakdown)
  - gradual drop in capacitance.
- The time-to-failure as a result of
  - **avalanche breakdown** was found to decrease with an *increase* in the area of the capacitor.
  - **gradual drop in capacitance** was found to decrease with a *decrease* in the area of the capacitor

THB tests (85^{o}C and 85% RH with bias of 0, 5, and 150V):

- The capacitance of embedded capacitors was found to increase (about 15% in 395 hrs) during THB conditions due to moisture absorption.
- Failures due to a drop in insulation resistance were observed only at 85^{o}C/85% RH and 150 V in 395 hrs.

Future Work

Temperature and voltage aging:

- Compute the MTTF as a result of avalanche breakdown at 125^{o}C, 250 V and 105^{o}C, 285 V.
- Obtain the values of constants (n and E_a) of the Prokopowicz model.
- Model the time-to-failure of embedded capacitors as a result of decrease in capacitance during temperature and voltage aging.

Temperature-Humidity-Bias tests:

- Continue the THB test at 85^{o}C/85% RH, at 0 V and 5V bias until all capacitors fail or 2500 hrs (whichever is earlier).